UNIVERSITA' DEGLI STUDI DI PADOVA

DIPARTIMENTO DI MEDICINA MOLECOLARE

SCUOLA DI DOTTORATO IN RICERCA IN BIOMEDICINA
CICLO XXVIII

Immunological restoration in chronic HCV-infected patients treated with different antiviral therapies

Direttore della Scuola: Chiar.mo Prof. Stefano Piccolo
Supervisore: Prof.ssa Antonella Caputo

Dottoranda: Valentina Telatin

Anno Accademico 2017/2018

INDEX

SUMMARY OF THE STUDY

The World Health Organization (WHO) estimates that approximately 3% of the global population is chronically infected with Hepatitis C Virus (HCV) and that approximately 3-4 million new cases of hepatitis C occur each year worldwide. While African countries have the highest prevalence of HCV infection (up to 26%) in the world, however, HCV infection represents a global health challenge from which no country, rich or poor, is spared. The acute phase of HCV infection is asymptomatic in the majority of infected individuals (75-80%), and except few cases of acute hepatitis C followed by viral clearance, in approximately 80% of patients the virus establishes a chronic infection and, among these patients, about 20% develop cirrhosis with possible degeneration in hepatocellular carcinoma (HCC) in 1-5% of cases. At present, although numerous candidates have been pursued, there is no vaccine available to prevent HCV infection and, even if antiviral drugs are the choice of treatment, HCV infection indeed represents a major health problem worldwide.

New generation of highly effective interferon-free, direct acting antivirals (DAAs) therapies have been recently introduced in the clinical practice promising to cure HCV and to overcome the issues related to interferon-based therapies. DAAs have revolutionized the care of HCV-infected individuals due to their dramatically high cure rate, above 90%. Nonetheless, recent reports describe the presence of occult HCV infection in some patients, and the occurrence and recurrence of HCC, despite sustained virological response (SVR) after treatment with DAAs (Koutsoudakis G.et al., 2017; Elamarsy S. et al., 2017; Vukotic R. et al., 2017; Reig M. et al., 2016). In addition, the emergence of drug resistance and suboptimal activity of DAA-based therapies against different HCV genotypes have been observed, causing treatment failure and hampering the control of HCV spread globally (Pawlotsky J.M.et al., 2016; Gimeno-Ballester V. et al., 2017). For all these reasons, and considering also that a previous HCV cleared infection does not ensure prevention from re-infection, at present it is unclear if HCV eradication worldwide will be achieved with DAAs therapies alone or with the combination with immunotherapies.

Mechanisms regulating viral clearance or establishment of chronic infection and disease progression have been clarified only partially and several questions are still open (Manns M.P. et al., 2017). During HCV chronic infection, HCV-specific $CD8^+$ T lymphocytes are present in the liver, but these cells are not able to control the replication of HCV, because they have lost their antiviral effector functions, such as cytokine production, proliferation and cytolytic activity. Recent hypothesis is that the loss of function of T lymphocytes may be due to both

the liver microenvironment and other cell populations such as $CD4^+$ regulatory T cells (Tregs) or myeloid-derived suppressor cells (MDSCs) exerting inhibitory functions and favoring viral escape and disease progression. MDSCs have been well described in multiple severe human diseases such as cancer, autoimmune diseases, and infections but little is known on their role in HCV infection.

A hallmark feature of persistent HCV infection is chronic immune activation and dysfunction of several types of immune cells, including naïve and memory $CD4^+$ and $CD8^+$ T cells, which have been linked to perturbation of anti-viral and anti-tumoral immune responses. Besides, HCV may exert direct effects on B and T lymphocytes and accelerate T cell immune senescence, as the presence and replication of HCV in these cells has been reported, contributing to viral persistence and impairing overall immune responses and vaccination against other infectious agents. Therefore, the global dysregulation of the immune system caused by HCV infection, in addition to affect HCV clearance itself, may be deleterious in terms of response to other infectious agents and tumor onset.

In this context, how DAA treatments influences immune responses and immune activation, and whether effective inhibition of HCV replication by DAAs restores defective innate and adaptive immune responses in HCV chronically infected patients are unclear and require further investigation. Recent evidence indicate that, in patients with SVR after interferon-free DAA treatments, HCV clearance was associated with improved blood HCV specific immunity (Spaan M. et al., 2016; Serti E. et al., 2015; Larrubia J.R. et al., 2015; Burchill M.A. et al., 2015). However, contradictory results have been reported for MDSCs and other recent studies indicate that DAA-induced HCV clearance does not completely restore the altered cytokines profile in T lymphocytes and $CD4^+$ Treg cells frequency and activation status (Hengst J. et al., 2016; Langhans B. et al., 2017), implying that HCV cure does not lead to complete immune reconstitution and that regulatory cells may play a role in progression of liver disease even long-term after HCV cure. This issue is of crucial interest in the development of strategies aimed at eradicating HCV infection. Indeed, the incomplete reconstitution of HCV-specific and non-specific immune responses even after DAAs treatment may lead to the occult HCV infection and the development of HCC despite SVR (Koutsoudakis G. et al., 2017; Elamarsy S. et al., 2017; Vukotic R. et al., 2017; Reig M. et al., 2016).

To gain further insights into the activity of DAAs on the immune dysfunction, the main objective of this study is to evaluate the capacity of DAA treatments of restoring immune functions, focusing on features of cellular responses known to be affected by HCV infection and/or to be crucial for the effectiveness of adaptive immune responses, such as: 1) the evaluation of the presence, frequency and function of suppressive regulatory cells, including MDSCs. I have focused my attention on M-MDSCs as other reports already

showed an increase of this monocytical population in patients infected by HCV, while the effects of HCV antiviral DAA-based treatments on frequency and phenotypes of these cells remain unknown; 2) the phenotype of different $CD4^+$ and $CD8^+$ T cell subpopulations, including evaluation of chronic immune activation, exhaustion, and differentiation, and the presence of Treg, that in other contexts have been shown to be affected by chronic immune activation (Maue A.C. et al., 2009; Papagno L. et al., 2004; Sforza F. et al., 2014); and 3) some metabolic properties of different $CD4^+$ and $CD8^+$ T cell subpopulations. T cell metabolism drives lymphocyte functionality, and may be affected by chronic infections (Dimeloe S. et al., 2016). However, no data are available for HCV infection.

Finally, since in the last years several studies demonstrated the regulatory role of microRNAs (miRNAs) in gene expression and their implication in HCV replication and in MDSCs expansion, I have also analysed the expression profile of miRNA-122, miRNA-196b, miRNA-21 and miRNA-29a (known to play a role in HCV replication and in the expansion of myeloid progenitors) as possible biological markers in peripheral blood of selected HCV infected patients under different therapies or untreated.

For the purpose of this study I have enrolled a total of 262 HCV-chronically infected patients, grouped in: 1) untreated (n=75); 2) during different pharmacological therapies (n=70) (IFN-based n=10, and IFN-free n=60); 3) with cleared infection after the end of pharmacological therapy (n=115) (IFN-based n=38, and IFN-free n=77); 4) patients who have spontaneously cleared HCV infection (n=2) and 5) healthy controls (n=47).

The main results of the study demonstrates that M-MDSCs are deeply altered by HCV infection both quantitatively and qualitatively, and that this is part of a more general phenomenon of HCV-induced immune dysregulation involving also $CD4^+$ and $CD8^+$ T cell subsets. In addition, the results indicate that DAA-based therapy only partially, and slowly, restores these phenomena.

1. INTRODUCTION

1.1 Overview and epidemiology of HCV infection

Hepatitis C virus (HCV) causes both acute and chronic infections which are asymptomatic in approximately 80% of patients. After the acute infection, only 15%-25% of the patients became cured spontaneously and 75%-85% develop chronic infection with the diagnosis made if viremia persists 6 months from the onset. According to reports of the World Health Organization (WHO) (www.who.it), 15-30% of chronic infections progress to cirrhosis of the liver, and eventually, 1-5% of those cirrhotic patients develop hepatocellular carcinoma (HCC) within 30-40 years (Barth H., 2015).

Usually, HCV spread through the transfusion of unscreened blood and blood products and sharing, reuse or inadequate sterilization of injection and medical equipment. Although more rare, HCV can also be transmitted sexually and from an infected mother to her children. According to WHO estimates, in 2015 there were 1,75 million new HCV infections globally.

Due to the high replicative activity of HCV and to the lack of a proof-reading ability of viral RNA-dependent RNA polymerase (NS5B), there are multiple strains (or genotypes) of circulating HCV virus, whose distribution varies by region. HCV isolates are classified into seven major genotypes that differ in their nucleotide sequence by 30-55% and, within some HCV genotypes, in several subtypes (designed as a, b, c, and so on) differing in their nucleotide sequence by 20-25% (Moradpour D. et al., 2007) and in *quasispecies* (genomes with minor genetic differences that continue evolve within the same individual) (Halfon P. and Locarnini S., 2011). It is estimated that 130-170 million people are infected by HCV worldwide. The distribution of HCV infection is highly variable, with the highest prevalence in Africa and in the Middle East and a lower prevalence in the Americas, Australia and Northern and Western Europe. China has the largest number of HCV-infected individuals with 29,8 million, followed by India (18,2 million) and Indonesia (9,4 million) (Hajarizadeh B. et al., 2013).

Recent data indicate that HCV genotype 1 is the most prevalent worldwide, comprising 83,4 million cases (46,2% of all HCV cases) of which one-third in East Asia. It is also the genotype most prevalent in the developed countries. Genotype 3 is the next most prevalent HCV genotype globally, with 53,3 million cases (30,1%), three-quarters of which occur in South Asia. Genotypes 2, 4, and 6 are responsible for a total 22,8% of all cases. East Asia accounts for the greatest numbers of genotype 2 and 6, while genotype 4 is the most prevalent in North

Africa and Middle East. Genotype 6 is endemic in Southeast Asia and is highly prevalent in Honk Kong and Southern China, whereas genotype 5 comprises the remaining <1% of HCV cases globally, with the greater majority of which in Southern and Eastern sub-Saharan Africa. The genotype 1 and 3 dominate in most countries irrespective of economic status and the largest proportions of genotype 4 and 5 are in lower-income countries. Finally, the genotype 7, originating from central Africa, is the one that has been more recently discovered **(Figure 1)** (Messina J.P. et al., 2015).

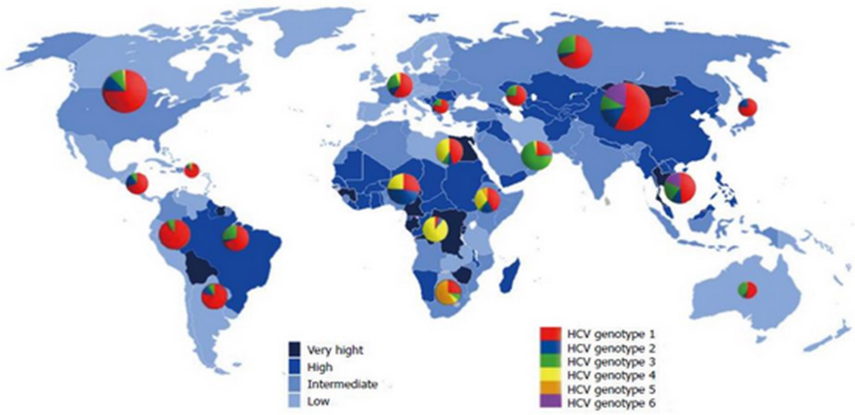

Figure 1: Overall prevalence of hepatitis C virus infections and the distribution of different hepatitis C virus genotypes worldwide (Daw M.A. et al., 2016).

1.2 HCV structure and genome organization

HCV is a small enveloped virus with a spherical morphology of approximately 40-70 nm in size which belongs to the family of *Flaviridae*. It contains a 9,6 kb positive-strand RNA genome flanked by non-translated regions (NTRs) at both C- and N- terminals (**Figure 2**) (Bowen D.G. and Walker C.M., 2005; Lauer G.M., 2013; Fournier C. et al., 2013). The 5'-NTR is highly conserved among the different HCV isolates and is important for viral RNA replication and translation. This region contains the Internal Ribosomal Entry Site (IRES) sequence required for translation of the HCV RNA genome yielding a polyprotein precursor that is processed by cellular and viral proteases into the mature structural and non-structural proteins.

The HCV structural proteins (the capsid 'core' protein and the glycoproteins, E1 and E2) map at the N-terminal region of the polyprotein, whereas the non-structural (NS) proteins (p7, NS2, NS3, NS4A, NS5A, and NS5B) map in the C-terminal of the polyprotein (Huang L. et al., 2004; Steinmann E. et al., 2008; Halfon P. and Locarnini S., 2011).

The structural proteins form the viral particle include the core protein and the envelope glycoproteins E1 and E2. The glycoproteins **E1** and **E2** (33-35 and 70-72 kDa, respectively) are embedded in a lipid bilayer surrounding the nucleocapsid which is composed by the core protein and the RNA genome. The E1, E2 are hypervariable glycoproteins and associated with the endoplasmic reticulum (ER) within the cells. The envelope proteins are of great interest because of their potential use in the development of HCV vaccines (Khan A.G. et al., 2014), although their variability is challenging for the generation of effective neutralizing antibodies (Khan A.G. et al., 2014).

The **core protein** (~21 kDa) is composed of two domains: the N-terminal domain 1 (D1) and the C-terminal domain 2 (D2). D1 is a hydrophilic domain containing a high proportion of basic aminoacids and three nuclear localization signals implicated in promoting nucleocapsid assembly. D2 is mainly responsible for the association of the viral protein with cellular membranes, such as the membranes of the endoplasmic reticulum (ER). The core protein is highly conserved and plays multiple functions such as viral assembly, gene transcriptional regulation (Zuniga E. et al., 2015), apoptosis, alteration of IFN signalling, cell transformation and interference with lipid metabolism (Singaravelu R. et al., 2015). The HCV core protein localizes in the cell cytoplasm and in the nucleus (Steinmann E. et al., 2008).

The non-structural proteins include the p7 ion channel, the NS2 protease, the NS3-4A complex, the NS4B, the NS5A and, finally, the NS5B RNA-dependent RNA polymerase (RdRp), and are associated with viral replication and immune evasion (Lassmann B. et al., 2013).

p7 is an integral membrane polypeptide forming hexamers or heptamers with cation activity, and is thought to have an important role in viral particle maturation and release (Moradpour D. and Penin F., 2013).

NS2 is a serine protease responsible for the cleavage of NS2/3 (Shiryaev S.A. et al., 2012) and might be involved in viral assembly and release. It can also bind host pro-apoptotic protein CIDE-B, which subsequently inhibits apoptosis (Guglietta S. et al., 2009).

The **NS3-4A complex** localizes into the ER. It contains the multifunctional NS3 protein that is dispensable for RNA replication due to the serine protease domain, located in the N-terminal region, and the RNA helicase domain, located in the C-terminal region of the protein. NS4A is a cofactor for the NS3 serine protease. The NS3-4A complex is also responsible for cleavage of the HCV precursor polypeptide into individual proteins and is essential for virion assembly. In addition, it inhibits the innate immune response favouring HCV persistence (Heim M.H. and Thimme R., 2014; Enomoto H. et al., 2016).

NS4B is a hydrophobic integral membrane protein that induces alterations of intracellular membranes, designed the membranous web, which are thought to be the site of viral RNA replication.

The highly phosphorylated protein **NS5A** is phosphorylated by cellular serine kinases, including MEK1, MKK6, AKT, p70S6K, and cAMP-dependent protein kinase A-a.42-46 and is associated with the ER membrane (Hamamoto I. et al., 2005). It is required also for replication and interferes with type I interferon pathway favouring virus persistence (Macdonald A. and Harris M., 2004; Huang L. et al., 2005; Moradpor D. and Penin F., 2013).

Finally, the **NS5B** is a RNA-dependent RNA polymerase (RdRp) required for HCV RNA replication (Heim M.H. and Thimme R., 2014). It interacts with viral and host proteins, the interaction with NS3 and NS5a plays an important role in the HCV replication complex formation. This protein leads to the synthesis of a complementary negative-strand RNA using the genome as template. The genome with negative polarity is then the template for synthesis of the positive-strand RNA.

The 3'-UTR includes a minimal poly (U) tract of about 25 bases that is essential for replication.

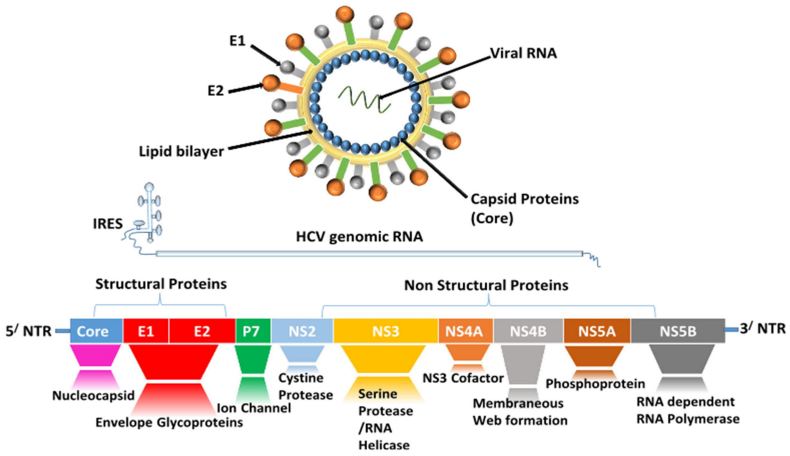

Figure 2: The HCV genome consists of a 9,6 kilobases single-strand RNA sequence flanked by 5'and 3' non-translated regions (NTR). IRES-mediated translation of the RNA produces a polyprotein that is processed by cellular and viral proteases into ten viral proteins: C, E1 and E2 structural proteins, and p7, NS2, NS3, NS4A, NS4B, NS5A and NS5B non-structural proteins. Abbreviations: C: Core protein, IRES: Internal ribosome entry site, E1 and E2: Envelope glycoproteins 1 and 2, NS: Non-structural protein (Elberry M. H. et al., 2017).

1.3 HCV replication cycle

The HCV replication cycle consists of 5 stages: viral entry, protein translation, RNA replication, virion assembly and release (**Figure 3**). The viral cycle starts with the binding of the HCV envelope glycoproteins to different receptors, including the tetraspanin protein CD81 (Rajesh S. et al., 2012), the

scavenger receptor class B type I (SRB1) (Yamamoto M. et al., 2011), glycosaminoglycans, the LDL receptor (LDLR) (Yamamoto M. et al., 2011) and claudin-1 (Yamamoto M. et al., 2011; Zeisel M.B. et al., 2011). Following clathrin-mediated endocytosis and fusion between the viral envelope and the endosome membrane, the nucleocapsid is released into the cytoplasm. The viral genome is then uncoated and transported to the ER where translation occurs (Friebe P. and Bartenschlager R., 2009; Pham T.N. et al., 2010). The IRES sequence guides the translation process leading to the polyprotein precursor of approximately 3000 aa, that is co- and post-translationally processed by cellular (ER signal peptidases) and viral proteases (NS2/3 protease and the NS3/4A serine protease) into the mature structural and non-structural proteins. After RNA translation, the RNA synthesis starts. Virions presumably form by budding into the ER, or into an ER-derived compartment, and exit the cell through the secretory pathway, thus acquiring the external envelope from intracellular membranes (Moradpour D. et al., 2007; Steinmann E. et al., 2008; Fournier C. et al., 2013).

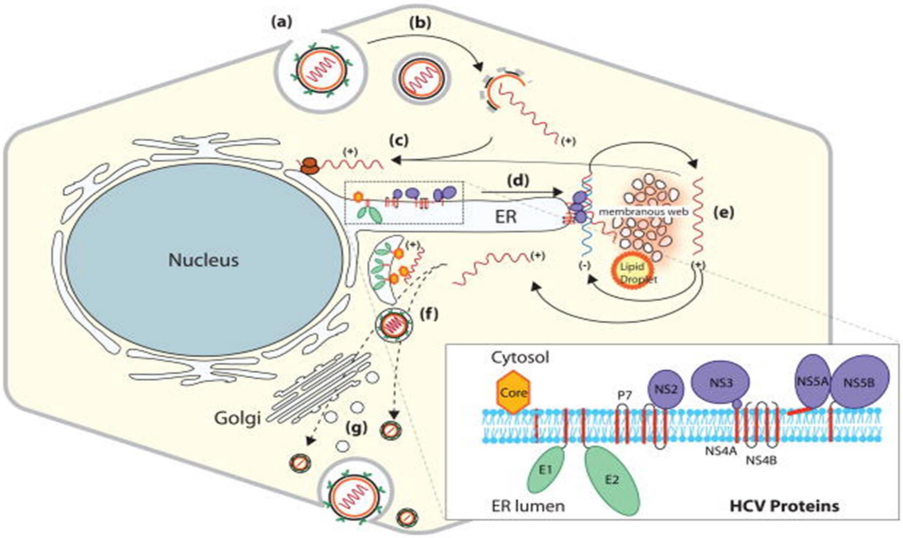

Figure 3: The viral life cycle is illustrated in steps a-g. (a) HCV enters hepatocytes via putative receptors. (b) pH-dependent fusion of the viral envelope and uncoating of genomic RNA occurs in endosomes, followed by (c) IRES-mediated translation on the rough endoplasmic reticulum (ER). HCV proteins and their association in the ER are shown in the insert; next, (d) assembly of ribonucleoprotein complexes (RNP) occurs, and (e) these RNP complexes engage in RNA synthesis to produce (+) polarity viral RNAs. RNA synthesis is believed to occur in the HCV-induced membranous structures termed 'membranous web'. (f) + polarity RNAs are encapsidated, and (g) HCV maturation and release ensues. HCV virions traffic through the Golgi or bypass the Golgi network. The mechanistic details of steps 'f and g' are not fully characterized (Syed G.H. et al., 2010).

The high genetic variability of HCV virus is mainly due to the high replicative activity and to the lack of a proof-reading ability of viral RNA-dependent RNA polymerase (NS5B), which does not have exonuclease activity 3'-5' and is not able to repair the nucleotide incorporation errors during viral replication.

1.4 History of HCV natural infection

The hepatitis C virus is one example of a viral pathogen that is very successful in establishing persistent infections by evading the immune system. Only small number of infected individuals (15-20%) is able to clear the infection spontaneously. Strong $CD8^+$ and $CD4^+$ T cell responses are critical in HCV clearance, as well as cytokine-induced factors that can directly inhibit virus replication. In contrast, about 80% of the infected individuals develop a chronic infection (Spaan M. et al., 2012). In these persistently infected patients the symptoms are relatively mild or absent, and it may take decades before the serious consequences of chronic HCV infection become apparent (**Figure 4**).

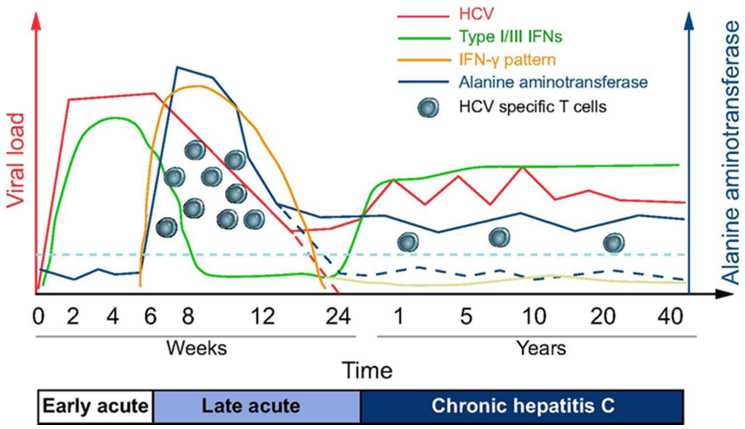

Figure 4: Schematic immune response in acute and chronic infection. The acute phase can be divided in an early phase prior to the activation and recruitment of HCV specific T cell in the liver and a late acute characterized by the adaptive immune response (Heim M. and Thiemme R., 2014).

The host reaction in the liver during the acute phase of HCV infection is characterized by strong host-response to HCV already few days after infection. The innate immune responses are induced within hours to days after infection (**Figure 4**) and provide the first line of defence against the invading viral pathogen. The host liver cells recognize the virus infection by the pathogen recognition receptors (PRRs), such as toll-like receptor (TLR), retinoic acid inducible gene-1 (RIG-1) and melanoma differentiation antigen 5 (Mda5), resulting in the rapid production of pro-inflammatory cytokines (e.g. TNF and IL-6) and antiviral type I and III

interferons (IFNs) (Heim M.K. and Thiemme R., 2014). Interferons are cytokines responsible for the induction of an antiviral state by the up-regulation of IFN-stimulated genes (ISGs), expression of multiple antiviral effector proteins and activation of immune cells, including natural killer (NK) cells and T cells. Indeed, patients with genetic defects in the IFN system frequently die of viral diseases at an early age (Thiemme R. et al., 2012). The NK cells are able to release IFN-γ and to kill virus-infected cells via cytotoxic molecules (e.g. perforin and granzymes) or via cytokines (e.g. IFN-γ and TNF) leading to suppression of the viral replication as well as to activation of adaptive immune responses (Spaan M. et al., 2012). Then, there are dendritic cells (DCs) whose activation occurs after encountering with pathogen. Their main function is to present the antigen to $CD4^+$ helper T cells in the lymph nodes, and therefore the latter begin to proliferate and produce cytokines, such as IL-2, IFN-γ or IL-4, that are required for the development of cytotoxic $CD8^+$ T cells.

The adaptive immune response is detectable approximately 6-8 weeks after infection (**Figure 4**) and plays a central role in the control of HCV infection. In fact, spontaneous viral clearance is associated with an early neutralizing antibody response as well as vigorous and sustained HCV-specific $CD4^+$ and $CD8^+$ T cell responses (Neumann-Haefelin C. and Thiemme R., 2013).

It seems that a well-coordinated interaction of the different immune cells is essential for a successful immune response against HCV but little is known about the precise interaction of this cross-talk.

The persistence of viral infection is due both to the generation of viral escape mutants and to the ability of the viral proteins to dysregulate, very early during infection, innate and adaptive immunity by hampering IFN production, skewing the differentiation of $CD4^+$ T cells toward unfavourable subsets, such as regulatory T cells (Treg), impairing the function of cytotoxic $CD8^+$ T cells and suppressing the function of NK cells, thus favouring the establishment of viral persistence.

The expression of the polyprotein as well as the single HCV proteins antagonizes the antiviral effect in different ways (Kumthip K. and Maneekarn N., 2015).

The HCV core protein is secreted from HCV-infected hepatocytes and present extracellularly in the plasma of chronic patient (Tacke R.S. et al., 2012). At this level the core protein exerts an immunomodulatory role in human monocytes/macrophages and DC cells resulting in inhibition of proinflammatory cytokine production and in the activation of the transcription factor STAT3 that is critical for the development of regulatory APCs, through the up-regulation of IL-6 (Tacke R.S. et al., 2012).

HCV proteins are responsible for the inhibition of IFN-mediated antiviral effects. For example, HCV blocks the RIG-I signalling through the actions of the NS3/4A protease *in vitro* (Chung R.T. et al., 2008). Additionally, it has been described the inhibitory effect of core and NS4B proteins on IFN-induced phosphorylation and nuclear translocation of STAT1 in cell cultures and the involvement of E2 protein in mediating IFN-α resistance through the inhibition of protein kinase R (Kumthip K. and Maneekarn N., 2015).

Moreover, it was shown that HCV infected patients have a defect in HCV-specific neutralizing antibodies, directed against "hot spot" regions in and adjacent to hypervariable region 1 of the envelope glycoproteins E1 and E2, and essential for preventing viral infection and spread. HCV also escape the virus-specific $CD8^+$ T cell response due to different types of mutations, such as in the HLA I binding anchors of $CD8^+$ epitopes (Neumann-Haefelin C. and Thiemme R., 2013).

Furthermore, another hallmark of chronic infection is the T cell dysfunction which prevent accelerated liver damage lacking the symptoms in the majority of chronic HCV patients. The slower progression of liver disease is another consequence of weak T cell responses (Spaan M. et al., 2012). However, these dysfunctional HCV-$CD8^+$ T cells have been shown to be impaired in cytotoxicity, production of antiviral cytokines, and antigen-triggered proliferation and are characterized by an exhaustive phenotype including PD-1, Tim-3, CTLA-4, 2B4, CD160 and KLRG1. Finally, in chronic hepatitis C, $CD4^+$ T-cell responses are weak or even absent (Neumann-Haefelin C. and Thiemme R., 2013).

1.5 Pharmacological treatment of HCV infection

In the absence of an effective prophylactic or therapeutic vaccine against HCV infection, at present the only mean to treat HCV infected individuals is the use of drugs.

Before the identification of HCV, from 1986 to 1998 the standard care of hepatitis C was interferon-α (IFN-α), that remained an essential component of effective treatment regimens in the 25 years that followed. However, the IFN-α monotherapy showed relevant side effects as well as a sustained virological response (SVR), defined as the absence of detectable HCV RNA 6 months after the end of the therapy, of only 15-20% and efficacy only against some genotypes (Heim M.K., 2013).

In the late 1998s, the new standard of care became the combination therapy of IFN-α plus ribavirin (RBV), a nucleoside analogue that has a broad range of antiviral activities. A study that included 912 patients showed that the combination of subcutaneously injected IFN-α with daily oral administration of RBV led to more than 20% of SVR compared with IFN-α monotherapy (Heim M.K., 2013).

In 2001, after the conjugation of IFN-α with a polyethylene glycol (PEG) chain, the SVR increased up to 40-50% for genotype 1 and 70-80% for genotypes 2 and 3 (Yau A.H.L.Y. and Yoshida E.M., 2014). The administration of this therapy for 6 to 12 months (depending on the HCV genotype) became the standard of care protocol for the subsequent 10 years.

The limited safety and tolerability of IFN-based regimens and their effectiveness only against some genotypes and the current understanding of the HCV viral life cycle have led in the recent years to the development of novel effective drugs targeting specific HCV enzymes and proteins, which were therefore named direct-acting antivirals (DAAs). These drugs act on the NS3/4A protease (e.g. telaprevir, boceprevir, simeprevir and paritaprevir), NS5B RNA-dependent polymerase (e.g. sofosbuvir, daclatasvir and dasabuvir) and the NS5A serine protease (e.g. ombitasvir and ledipasvir) (**Figure 5**), blocking virus replication and inducing progressive viral clearance very effectively (Horsley-Silva J.L. et al., 2017).

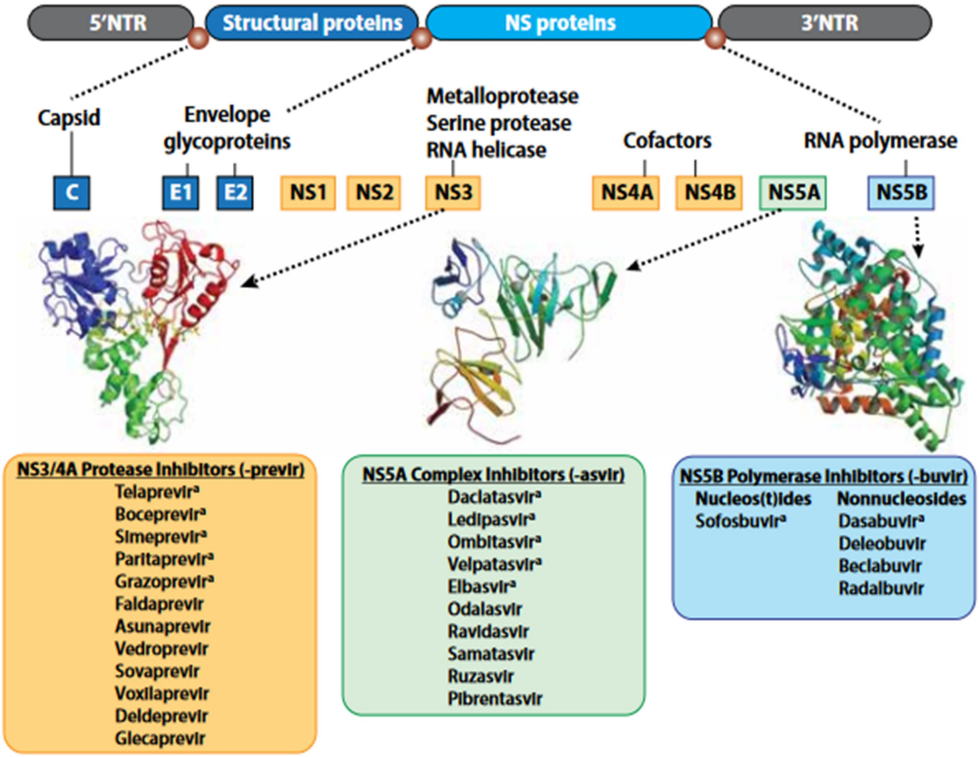

Figure 5: The RNA genome of HCV encodes several non-structural proteins (NS) essential for virus replication which are the targets of new DAAs. A NS3/4A serine protease cleaves unprocessed polyproteins to create functional, individual proteins, a process blocked by protease inhibitors (-previr). The NS5A protein helps with HCV RNA replication regulation and viral assembly and packaging, and directly interacts with the RNA-dependent RNA polymerase (RdRp). NS5A inhibitors (-asvir) prevent hyper-phosphorylation of the NS5A protein and alter the protein's location from the endoplasmic reticulum. NS5B polymerase inhibitors (-buvir) work broadly against genotypes with intermediate potency and have a high barrier to resistance. Nucleos(t)ide inhibitors arrest RNA synthesis, while non-nucleoside inhibitors bind and disrupt the RdRp function (Horsley-Silva J.L. et al., 2017).

Telaprevir and boceprevir were the first DAA agents approved in 2011; these NS3/4A protease inhibitors were initially used in combination with PEG-IFN plus RBV; however, these are effective only against HCV genotype 1 infection, and have a low barrier to resistance. The patients cure rates with this new triple therapy increased from around 20-30% to 70-80% with a reduction of time of treatment (Delegan L. et al., 2013).

Few years later, these two drugs were outpaced by three new DAAs: sofosbuvir, a pan-genotypic nucleotide NS5A polymerase inhibitor, which was the first interferon-free option for HCV genotypes 2 and 3 and in combination with PEG-IFN plus RBV for the others; simeprevir, a first-generation NS3-4A protease inhibitor active against genotypes 1 and 4, and daclatasvir, a pan-genotypic NS5A inhibitor. Each of these DAAs was initially used as a component of a triple

combination regimen with PEG-IFN-α and RBV, yielding SVR rates of 90-95% (Welzel T.M. et al., 2014).

The development of IFN-free combinations of direct-acting antiviral agents have been shown to have not only a better impact on viral clearance and SVR but also on health-related quality of life. Of note, the multi-targeted therapy based on three DAA, the protease inhibitor ABT-450 with ritonavir (ABT-450/r), the NS5A inhibitor ombitasvir (ABT-267), the nonnucleoside polymerase inhibitor dasabuvir (ABT-333), and ribavirin, in an open-label phase 3 trial involving previously untreated and previously treated adults with HCV genotype 1 infection and compensated cirrhosis resulted in high rates of SVR without adverse events (Poordad F. et al., 2014).

The different genotypes of HCV differ in their response to treatment with IFN-based or IFN-free therapies. For this reason, the identification of the infecting genotype has a significant importance for prognostic and predictive purposes, but with the approval of the combination sofosbuvir-velpatasvir in 2016, clinicians now have treatment options that achieve a SVR 12 week in patients with any HCV genotype characterized by short duration of the therapy (8-12 weeks) and low pill burden (Horsley-Silva J.L. et al., 2017).

Finally, the U.S. Food and Drug administration (FDA), in August 2017, has approved a new protocol named Mavyret (glecaprevir and pibrentasvir), which represents the first 8 week treatment for treatment of adults with chronic HCV infection with genotypes 1-6 (www.fda.gov).

1.6 Myeloid-derived suppressor cells (MDSCs)

Myeloid-derived suppressor cells (MDSCs) represent a population of tolerogenic and immune-suppressive myeloid cells with heterogeneous morphology, surface phenotype and function, but with immunosuppressive properties in common. Natural suppressor cells (the initial name for MDSC) were described more than 25 years ago in cancer patients and their crucial role in the inhibition of immune responses during some pathological diseases was shown only few years later (Talmadge J.E. and Gabrilovich D.I., 2013).

Immunosuppressive myeloid cells are most likely generated as a normal physiological response to acute and excessive inflammatory conditions (Millrud C.R. et al., 2017) and play key roles in the cellular network that regulate immune responses. One of the hallmarks of MDSCs is their ability to regulate innate immune response by modulating the cytokine production of macrophages and to suppress T-cell responses. These cells can accumulate within tumours, in lymphoid organs (e.g. spleen and bone marrow) and in peripheral blood. In healthy individuals MDSCs are present in low numbers in the blood, whereas during

pathological conditions they rapidly expand, such as in case of cancer, autoimmune or infectious diseases, trauma, sepsis and bone marrow transplantation.

The origin of MDSCs is due to a partial block in the differentiation pathway of immature myeloid cells into mature cells that occurs in pathological conditions and is associated with the loss of expression of cell-surface markers specifically expressed by monocytes, macrophages or dendritic cells (**Figure 6**). Instead, in healthy individuals the immature myeloid cells generated in the bone marrow quickly differentiate into mature cells (Gabrilovich D.I. and Nagaraj S., 2009).

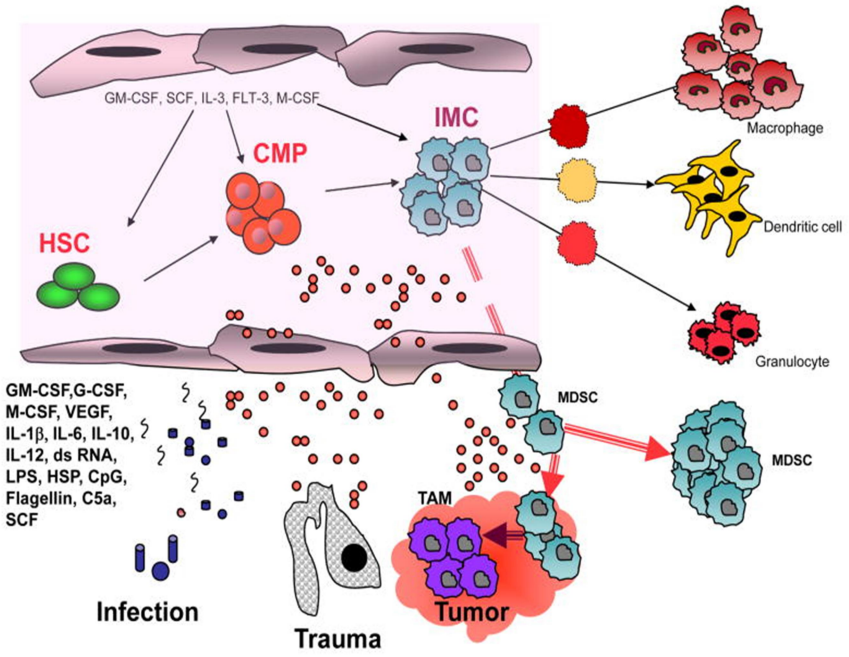

Figure 6: Origin of MDSCs. Immature myeloid cells (IMCs) are part of the normal process of myelopoiesis, which takes place in the bone marrow and is controlled by a complex network of soluble factors that include cytokines, such as granulocyte/macrophage colony-stimulating factor (GM-CSF), stem-cell factor (SCF), interleukin-3 (IL-3), FMS-related tyrosine kinase 3 (FLT-3), macrophage colony-stimulating factor (M-CSF) and cell-expressed molecules including Notch (not shown). Haematopoietic stem cells (HSCs) differentiate into common myeloid progenitor (CMP) cells and then into IMCs (Gabrilovich D.I., 2009).

MDSCs have been identified in most patients and experimental mice with tumours. From early observation MDSC phenotype in mice was initially defined on the basis of the co-expression of the CD11b (also known as αM-integrin) and Gr-1(Glutathione reductase) markers (Bronte V. et al., 1998; Gabrilovich D.I., 2013), and then later on the expression of several other surface markers. More recently, on the basis of expression of Gr-1/Ly-6G/Ly-6C and CD49d, two main subsets of MDSCs were described: 1) $CD11b^{+}/LY6G^{+}/LY6C^{low}$cells, characteristic of the granulocytes or the polymorphonuclear (G-MDSCs or PMN-MDSCs) fraction, and

2) $CD11b^{+}/LY6G^{-}/LY6C^{high}$ cells which refers to the monocyte fraction (M-MDSC) (Haile L.A. et al., 2010; Gabrilovich D.I., 2017).

The identification of human MDSCs is more complicated because of the lack of specific mature myeloid markers and of a human homologue of the mouse Gr-1 molecule.

Like mouse MDSCs, human MDSCs include monocytic and polymorphonuclear subsets characterized by a combination of several myeloid markers. Additionally, an immature subset of human MDSCs has been characterized by the absence of staining for the lineage markers (CD3, CD19, CD57 and MHC class II molecule HLA-DR) and expression of common myeloid markers CD11b and CD33 (Solito S. et al., 2014).

Therefore, criteria for phenotyping characterization of these cells by flow cytometry are now relatively well defined (Mandruzzato S. et al., 2016). PMN-MDSCs are defined as $CD11b^{+}/HLA\text{-}DR^{-}/CD33^{+}/CD14^{-}/CD15^{+}$ cells, although in most cases these markers have defined subsets of more mature and immature neutrophils that, according to recent data, can be distinguished by the differential expression of Lectin-type oxidized LDL receptor (LOX-1). The latter marker is practically undetectable in neutrophils in peripheral blood of healthy donors, whereas it is expressed in PMN-MDSC together with CD16 (Gabrilovich D.I., 2017; Bronte V. et al., 2016; Condamine T. et al., 2016). In particular, the use of antibodies against CD16 seems to separate neutrophils that are $CD16^{+}$ from the immature MDSCs $CD16^{low/-}$ (Damuzzo V. et al., 2015). Instead, M-MDSCs are defined as $CD11b^{+}/HLA\text{-}DR^{low/-}/CD33^{+}/CD14^{+}/CD15^{-}$. In addition, IL-4α chain receptor (IL-4Rα or CD124) has been suggested to be correlated with tumour derived MDSCs (Mandruzzato S. et al., 2009). Until today, however, the best marker for human MDSCs remain their suppressor functions that are described below.

Accumulation of MDSCs is a complex phenomenon. The main model that describe this process requires two distinct, although partially overlapping, signals: the first is responsible for the expansion of immature myeloid cells associated with inhibition of their terminal differentiation, and the second is responsible for the pathologic activation of these cells, converting immature myeloid cells to MDSCs (Condamine T. and Gabrilovich D.I., 2011).

The first group of signals is mostly produced by tumor cells and include: cyclooxygenase 2, prostaglandins, stem-cell factor (SCF), IL-6, macrophage colony-stimulation factor (M-CSF), granulocyte/macrophage colony-stimulation factor (GM-CSF) and vascular endothelial growth factor (VEGF). Most of these factors trigger the signalling pathways of JAK and STAT3, which is the main transcription factor that regulates the expansion of the MDSCs, and whose

abnormal and persistent activation prevents the differentiation of these cells in mature myeloid cells and promotes their expansion.

The second group of signals involved in the activation of MDSCs is produced by T cells and tumor stromal cells after induction by bacterial and viral products or tumor-cell death, and include IFN-γ, ligands for Toll-like receptors (TLRs), IL-4, IL-13 and transforming growth factor-β (TGFβ). These factors activate several signalling pathways in MDSCs that involve STAT6, STAT1 and NF-kB (Gabrilovich D.I., 2009).

The immunosuppressive activities of MDSCs require cell-to-cell contact through cell-surface receptors and/or through the release of soluble mediators. Several mechanism have been described (Solito S. et al., 2014). Two major catabolic enzymes metabolize L-Arginie and mediate MDSCs activity. These enzymes are arginase 1 (ARG1), which convert L-Arginine into urea and L-ornithine, and inducible nitric oxide synthase 2 (NOS2), which oxidizes L-Arginine to generate nitric oxide (NO) and citrulline (**Figure 7**) (Gabrilovich D.I. and Nagaraj S., 2009).

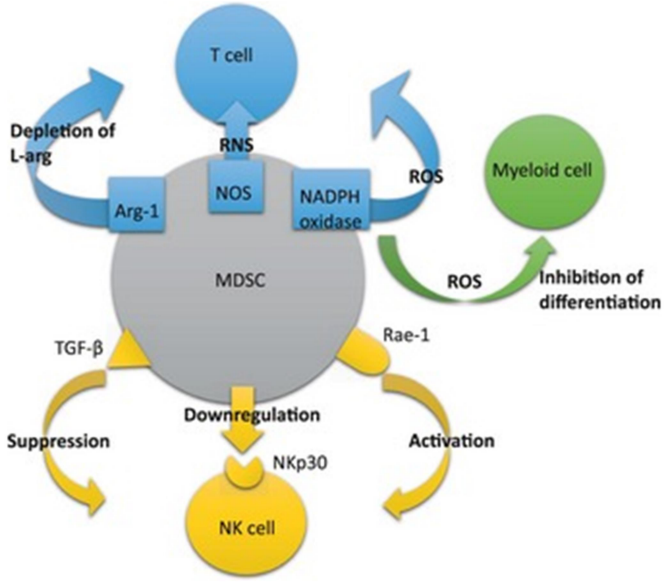

Figure 7: Molecular mechanisms of MDSC action on other immune cells. MDSCs suppress T cells, NK cells, and other myeloid cells via a variety of mechanisms. T cells appear to be mainly suppressed via the production of ROS and reactive nitrogen species (RNS) or via the depletion of L-arginine. On the other hand, MDSC-mediated inhibition of NK cell responses occur through either membrane-bound TGF-β or downregulation of NK cell activating receptor, NKp30. In contrast, to the immunosuppression of MDSCs on NK cell responses, MDSCs are also shown to activate NK cells. In addition, MDSCs act on myeloid cells and affect their differentiation in a ROS-dependent manner (Goh C. et al., 2013).

The expression of these two enzymes have a direct role in the inhibition of T-cell function. In particular, depletion of L-Arginine from the microenvironment

can lead to the production of H_2O_2, and both events inhibit expression of CD3ξ chain and, thereby, T cell proliferation, causing arrest of T cells in the G_0-G_1 phase of the cell cycle (Rodriguez P.C. and Ochoa A.C., 2008).

ROS production, mainly in the form of H_2O_2, is another mechanism used by MDSCs to inhibit T cell proliferation, and is induced by several factors, such as TGFβ, IL-3, IL-6, IL-10, PDGF and GM-CSF.

MDSCs can increase the presence of ROS by expressing NOX2, the catalytic subunit (also known as gp91phox) of NADPH oxidase, an enzyme that reduces oxygen to superoxide anions using electrons supplied by NADPH.

Another mechanism involved in ROS production by MDSCs is the combined activity of ARG1 and NOX2; when the availability of L-Arginine is limited by ARG1 activity, NOS utilizes molecular oxygen as principal substrate, producing superoxide anions. ROS are produced when superoxide anion interacts with NO and nitrate aromatic amino acids (such as tyrosine residues) in the T cell receptor (TCR) and CD8, resulting in a decreased recognition of peptide-MHC (major histocompatibility complex) by TCR (Rodriguez P.C. and Ochoa A.C., 2008).

A recent study of Goh C. and colleagues (2016), demonstrated that HCV infection induced MDSCs to suppress the production of IFN-γ by NK cells. They observed that NK cells co-cultured with HCV-conditioned $CD33^+$ PMBCs produced lower amounts of IFN-γ. The suppression was mediated by ARG1, as the supplement of L-Arginine showed an increment of MDSC ARG1 activity and the decrease of IFN-γ production.

In contrast to murine MDSCs, human MDSCs are not characterized by such clear differences in the mechanism of suppression. In murine models, for example, it is evident that granulocytic subsets of MDSCs exert their immunosuppressive effects via ROS, whereas the monocyte fractions produce ARG1 and NO via iNOS (Ostrand-Rosenberg S. et al., 2009). In humans, the granulocytic subset expresses high levels of ROS and low levels of NO, the monocyte subset expresses low levels of ROS and high levels of NO, whereas both subsets express ARG1 (Gabrilovich D.I. and Nagaraj S., 2009).

1.7 MDSCs and HCV infection

HCV infection dysregulates both innate and adaptive immunity by hampering IFN production, skewing the differentiation of $CD4^+$ T cells toward unfavourable Th2, Th17 and Treg subsets and impairing the function of cytotoxic $CD8^+$ T cells. HCV is known to suppress the function of NK cells, which play an important role in viral clearance and antigen-presenting cells (Goh C. et al., 2016).

Research on MDSCs in HCV infection is scarce and controversial. In patients with chronic HCV infection, Cai W. et al. (2013) reported that before PEG-IFN plus RBV therapy the number of peripheral blood MDSCs was higher than in healthy donors and that, after 4 weeks from the end of treatment, their level decreased and was positively correlated with lower levels of HCV RNA. Ning G. and colleagues (2015) reported that the number of monocytic-MDSCs (M-MDSCs) is higher than granulocytic-MDSCs (G-MDSCs) in HCV-infected patients and that the increase of the frequency of M-MDSCs correlates with the age, suggesting that HCV infection may favour proliferation of M-MDSCs. However, in contrast to these findings, Nonnenmann J. et al. (2014) did not find any significant difference between the percentage of MDSCs in peripheral blood of chronic hepatitis C (CHC) patients and healthy controls nor significant correlation between the percentage of MDSCs and viral loads.

MDSCs of CHC patients are poorly characterized compared to those derived from cancer patients. However, MDSCs in the blood of CHC patients were shown to be HLA-$DR^{low/-}$/$CD11b^{+}$/$CD33^{+}$ and able to inhibit T cell proliferation mainly by means of ARG1 (Cai W. et al., 2013) and ROS production (Tacke R.S. et al., 2012). Recent studies demonstrated also that the HCV core protein could induce the generation and accumulation of MDSCs from PBMC *in vitro* (Tacke R.S. et al., 2012). Pang X. and colleagues (2016) showed that the HCV core protein induces M-MDSC production from monocytes through the PI3K pathway and autocrine cytokines, such as IL-10, IFN-β and TNF-α. Finally, other researchers demonstrated that purified monocytes from healthy donors cultured with the HCV core protein or cell-derived HCV virions (HCVcc) induced expression of indoleamine 2,3-dioxygenase (IDO), PD-L1 and IL-10 and down-regulated HLA-DR expression in human monocytes (Zhai N. et al., 2017). Furthermore, it was shown that HCV induced MDSC-like suppressive monocytes induce expansion of $CD4^{+}$ $Foxp3^{+}$ regulatory T cell (Treg) and inhibit autologous $CD4^{+}$ T cell activation (Zhai N. et al., 2017). Recent studies indicate an increment in the frequency of the monocyte fraction as $CD14^{+}$HLA-$DR^{-/low}$ in peripheral blood of patients with several type of cancer, including hepatocellular carcinoma (HCC) (Solito S. et al., 2014). In HCC, the liver has been shown to be the site of accumulation of MDSCs during infectious and neoplastic diseases. Different hepatic cell types as well as liver-derived soluble factors have been implicated in the recruitment and differentiation of MDSCs under various conditions, such as hepatic stellate cells (Hammerich L. and Tacke F., 2015).

MDSCs in HCC patients are able to inhibit T cell proliferation in a ARG1-dependent manner and also indirectly by the induction of $CD4^{+}$/$CD25^{+}$/$Foxp3^{+}$ Treg suggesting a network of interactions between regulatory populations *in vivo*

(Hoechst B. et al., 2008). Finally, a recent study reports hypoxia as a cause of MDSC accumulation in HCC (Chiu D.K. et al., 2017).

Overall the results of these studies suggest that MDSCs may play a role in the progression of liver disease in patients with chronic HCV infection, but further studies are needed to better clarify the role of these cells in HCV-associated disease and during therapy.

1.8 miRNA

MicroRNAs (miRNAs) are single-stranded RNAs (ssRNAs) of 19-25 nucleotides in length generated from endogenous hairpin-shaped transcripts. The miRNAs function as molecules in post-transcriptional gene silencing by base pairing with target mRNAs, leading to mRNA cleavage or translational repression. With >200 members per species in higher eukaryotes, miRNAs are one of the largest gene families, accounting for about 1% of the genome. Recent studies have revealed that miRNAs have key roles in different regulatory pathways, including control of developmental timing, haematopoietic cell differentiation, apoptosis, cell proliferation and organ development (Chen S. et al., 2015). In various human diseases, an abnormal expression and function of these small RNAs has been observed (Santos J.M.O. et al., 2018).

miRNA genes are transcribed by RNA polymerase II (pol II) to generate the primary transcripts (pri-miRNAs) (**Figure 8**). The transcription of miRNA genes yields to a primary transcript called pre-miRNA containing a local hairpin structure. Pre-miRNA is processed in the nucleus by the large nuclear protein drosha, an RNase III enzyme, which cleaves the stem-loop structure releasing the precursor of miRNA: pre-miRNA. This precursor is transported into the cytoplasm by exportin-5, a nuclear transport receptors, through nuclear pore complexes embedded in the nuclear membrane. In the cytoplasm, pre-miRNA is processed to generate a mature double stranded short RNA of about 22 nucleotides by the enzyme dicer. The mature miRNA and dicer constitute the RNA-induced silencing complex (RISC), a multiprotein complex that includes members of the Argonaute protein family. Usually, only one stranded, called guide strand (functional strand), is incorporated in this complex, recognizes and binds the 3' untranslated region of target mRNA. The other non-functional strand is degraded. miRNA exerts its function by degrading the target mRNA if there is a perfect base pairing with the target or inhibiting mRNA translation if the there is a partial pairing (Kim V.N. et al., 2005).

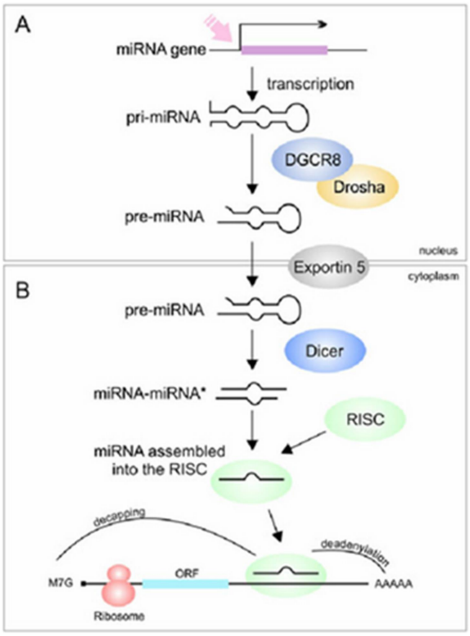

Figure 8: Scheme of microRNA biogenesis and action. (A) Nuclear step of miRNA biogenesis. (B) Cytoplasmic step of miRNA biogenesis (Gurianova V. et al., 2015).

1.9 miRNA and HCV infection

miRNA expression levels of patients with various diseases are dysregulated as compared to healthy controls (Santos J.M.O. et al., 2018; Xie K.L. et al., 2014); therefore, these molecules have attracted much attention in the last years as potential non-invasive biomarkers for screening and diagnosing various disease, including HCV infection.

The most abundant and the most studied is miR-122, which is abundant in liver cells, positively modulates HCV infection through direct interactions with the viral RNA and is required for HCV translation. Since miRNA-122 plays an essential role as host factor for HCV production, an acid-modified DNA phosphorothioate antisense oligonucleotide of miRNA-122, called miravirsen, was produced to suppress HCV replication. In addition, a decrease of miRNA-122 levels was shown after a combination of DAAs (Waring J.F. et al., 2016) confirming its important role for HCV replication.

Besides miR-122, other miRNAs have been involved in HCV replication. Overexpression of miR-448 and miR-196 were able to substantially attenuate viral replication by directly targeting core and NS5A coding region of the HCV genome, respectively. Let-7b was also identified as a novel cellular miRNAs that directly target HCV genome and elicits anti-HCV activity (Cheng J.C. et al., 2012). Mutational analysis identified let-7b binding sites at the coding sequences of NS5B and 5'-UTR of HCV genome that were conserved among various HCV genotypes.

Others miRNAs inhibit HCV replication directly, such as miRNA-196b that has a target site in NS5A and is induced by IFN (Hoffmann T.W. et al., 2012; Scagnolari C. et al., 2010), while others act indirectly by activating the IFN pathway, such as miRNA-130a. (Duan X. et al., 2013). In addition, recent studies suggest a role, in the liver, of the miRNA-29 family (miRNA-29a, -29b and -29c) in the defence of cells against HCV (Hoffmann T.W. et al., 2012).

Most recently, it was shown that miRNA-141 is induced by HCV infection and necessary for an efficient viral replication, as its depletion inhibits viral replication (Duan X. et al., 2013).

In recent years the attention was focused on circulating miRNAs, as different expression of 106 miRNAs (51 up-regulated and 55 down-regulated) was observed in serum of HCV-infected patients compared with healthy controls (Zhang S. et al., 2015). Circulating miRNAs have been demonstrated to be very specific and stable in human serum and plasma, and for these reason they may be used as biomarkers for detection and as predictive marker for liver disease progression in HCV infection.

Serum levels of miRNA-21, miRNA-122 and miRNA-223 are elevated in patients with HCC or chronic hepatitis. Xu J. and colleagues (2011) found an elevation of these three miRNAs in patients with HCC or patients with chronic hepatitis compared with healthy donors. They demonstrated that elevated miRNA-122 and miRNA-223 in the serum of patients might reflect liver injury but not tumour itself.

Another study on serum miRNA has demonstrated an elevated expression of miR-18a, miR-221, miR-222, and miR-224 in HCC patients as compared to chronic HCV patients and cirrhotic patients and a lower expression of miR-101, miR-106b, miR-122, miR-195 in HCC patients as compared to chronic HCV patients (Sohn W. et al., 2015).

1.10 miRNAs and MDSCs

Emerging evidence suggests that miRNAs play a regulatory role in MDSC development, expansion and function. For instance, miR-29a, miR-21 and miR-196b participate in myeloid progenitor expansion (Tian J. et al., 2014). In particular, miRNA-21 has been found to be upregulated during the induction of MDSCs *in vitro* and present at high levels *in vivo* from tumour-bearing mice (Li L. et al., 2014). Furthermore, a study by Chen S. et al. (2015) suggest that depletion of miR-155 and miR-21 inhibits STAT3 expression in MDSCs and may be beneficial for cancer immunotherapy. Finally, an interesting study by Ren J.P. and colleagues (2017) revealed that miR-124 is down-regulated in HCV-infected

patients and implicated in activation of STAT3 which is overexpressed in MDSCs from HCV patients.

2. AIM OF THE STUDY

To gain insights into the activity of DAAs on the immune dysfunction reported in chronic HCV-infected patients, the main objective of this study is to evaluate the capacity of DAA treatments of restoring immune functions. I have focused on features of cellular responses known to be affected by HCV infection and/or to be crucial for the effectiveness of adaptive immune responses, such as 1) the evaluation of the presence, frequency and function of suppressive regulatory cells, including MDSCs. I have focused my attention on M-MDSCs. 2) the phenotype of different $CD4^+$ and $CD8^+$ T cell subpopulations, including evaluation of chronic immune activation, exhaustion, and differentiation, and the presence of Treg, that in other contexts have been shown to be affected by chronic immune activation some metabolic properties of different $CD4^+$ and $CD8^+$ T cell subpopulations. T cell metabolism drives lymphocyte functionality, and may be affected by chronic infections. However, no data are available for HCV infection.

Finally, since in the last years several studies demonstrated the regulatory role of microRNAs (miRNAs) in gene expression and their implication in HCV replication and in MDSCs expansion, I have also analysed the expression profile of miRNA-122, miRNA-196b, miRNA-21 and miRNA-29a (known to play a role in HCV replication and in the expansion of myeloid progenitors) as possible biological markers in peripheral blood of selected HCV infected patients under different therapies or untreated.

3. MATERIALS AND METHODS

3.1 Patients

A total of 262 HCV-infected patients were enrolled in the present cross-sectional study. The HCV infected individuals were grouped as follows: 1) untreated patients with chronic HCV infection (n=75) (no therapy, NT); 2) patients with chronic infection during pharmacological treatment (n=70) (therapy, T); 3) patients with cleared infection after therapy (n=115) (pharmacologically cured, PC) 4) patients who have spontaneously cleared HCV infection (n=2) (spontaneously cured, SC).

Patients undergoing therapy and those pharmacologically cured were treated with different combinations of antiviral drugs with a prevalence of direct acting antivirals regimens (DAAs), as summarized in **Table 1**.

Table 1: Anti-HCV therapeutic protocols

Therapy	[a]T	[b]PC
Peg-IFN+RBV	3	18
Peg-IFN+RBV+Telaprevir	7	18
Peg-IFN+RBV+Boceprevir	0	3
Ombitasvir+Paritaprevir/Ritonavir+Dasabuvir+RBV	16	16
Ombitasvir+Paritaprevir/Ritonavir+RBV	5	2
Glecaprevir+Pibrentasvir	3	0
Elbasvir+Granzoprevir	5	0
Sofosbuvir+RBV	10	5
Sofosbuvir+Daclatasvir	9	2
Sofosbuvir+Ledipasvir+RBV	13	4
Sofosbuvir+Simeprevir+RBV	0	6
Sofosbuvir+Velpatasvir	1	0
Sofosbuvir+PEG-IFN+RBV	0	1

[a]T, under therapy; [b]PC, pharmacologically cured

Forty-seven HCV-negative healthy individuals were also enrolled as controls (HC).

The directing-acting antiviral agents are interferon-free therapies and include HCV protease and polymerase inhibitors or their combination. The NS3/4A protease inhibitors are: telaprevir, boceprevir, paritaprevir, simeprevir, granzoprevir and glecaprevir. The NS5A protease inhibitors are: ledipasvir, ombitasvir, elbasvir and pibrentasvir. The NS5B RNA-dependent RNA polymerase

inhibitors are: sofosbuvir, dasabuvir and daclatasvir. Ritonavir, an anti-retroviral protease inhibitor, is used as a pharmacologic booster for paritaprevir.

Male and female volunteers with a diagnosis of HCV infection were included in this study, while patients with HIV or HBV co-infections, with malignancy different from liver cancer, autoimmune diseases and pregnant women were excluded. Patients were enrolled at the Infectious and Tropical Disease Unit of the Azienda Ospedaliera of Padua after signing an informed consent. The study was approved by the Ethics Committee of the Azienda Ospedaliera of Padua (Prot. n. 3136/AO/14 approved on 5 June 2014).

3.2 Blood collection

From each participant, approximately 18 ml of peripheral blood were collected in three 6 ml plastic whole blood tubes with spray-coated K2EDTA for isolation of plasma and purification of total leucocytes. Each patient was identified with an ID code and only the following information were provided to us: type of treatment, values of aspartate aminotransferase (AST) and alanine aminotransferase (ALT), blood HCV RNA load, HCV genotype, age, sex, blood cell counts and stage of disease, as reported in the "Results" section.

3.3 Plasma collection

One of the three 6 ml whole blood tubes was centrifuged at 2500 rpm in a bench centrifuge (Heraeus Megafuge 1.0R, swinging buckets 7570F) for 7 minutes at room temperature. After centrifugation, 1 ml of plasma was centrifuged at 3000 rpm for 5 minutes to remove residual cells. The plasma supernatants were then transferred in cryovials (Simport), stored at -20°C overnight and the following day moved at -80°C until use.

3.4 Purification of total leucocytes and PBMCs

The isolation of total leucocytes and peripheral blood mononuclear cells (PBMCs) was performed no longer than 4 hours after blood collection.

For **total leucocytes purification**, blood was transferred in three 50 ml tubes (BD Falcon) and diluted 1:3 with the haemolysis's solution, to remove red blood cells (RBC). The haemolysis's solution, provided by the pharmacy of Azienda Ospedaliera of Padua, contains NH_4Cl (8,6g/l), $KHCO_3$ (1g/l), EDTA tetrasodium (0,037g/l). The tubes were incubated for 20 minutes, centrifuged at 1200 rpm for 7 minutes , removed very gently from the centrifuge without moving the leucocyte pellet and the supernatant was discarded. Each pellet was further diluted with 10 ml of haemolysis's solution to remove residual RBC. The three cell

suspensions were pooled in a single 50 ml conical tube, incubated for 10 minutes and then centrifuged at 1200 rpm for 7 minutes. The pellet was resuspended in 10 ml of 1X Dulbecco phosphate buffer saline (D-PBS) without calcium and magnesium (Gibco) and alive cells counted (see section "Cell count" below). An aliquot of fresh total leukocytes was analysed by FACS (as described in section 3.6). The remaining cells were pelleted at 1500 for 5 minutes and frozen in 90% fetal bovine serum (FBS) (Lonza) and 10% DMSO (Sigma-Aldrich) in liquid nitrogen.

PBMCs purification was obtained from whole blood by the Ficoll (GE Healthcare) density gradient purification method. Briefly, blood was transferred in 50 ml tubes (BD Falcon), diluted 1:1 with 1X D-PBS, gently overlaid onto 10 ml of Ficoll solution in 50 ml conical tubes and centrifuged for 20 minutes at 1800 rpm without brake. The PBMC white rings were collected, washed twice with 1X D-PBS without calcium and magnesium (Gibco) and counted by the Trypan blue exclusion dye method (see section "Cell count" below). The cells were then pelleted at 1500 for 5 minutes and frozen in 90% FBS and 10% DMSO in liquid nitrogen until use. All procedures were carried out at room temperature.

3.5 Cell count

The Trypan blue dye exclusion method allows counting alive cells because the Trypan blue molecule does not cross the membrane of intact viable cells, which remain colourless, whereas it selectively colours in blue dead cells. Cellular suspensions (10 µl) were stained with 90 µl of 0,4% Trypan blue solution (Gibco). Then, 10 µl of the mix was pipetted in a disposable glasstic slide 10 with grids (Hycor). The cell count of three sets was carried out using the 10X objective of a light inverted microscope (Zeiss).

3.6 *Ex vivo* phenotypic analysis by flow cytometry

3.6.1 Phenotypic analysis of M-MDSCs

The frequency and phenotype of myeloid-derived suppressor cells (MDSCs) from HCV-infected patients and healthy donors was analysed by flow cytometry on freshly isolated total leukocytes. The monocyte fraction of MDSCs (M-MDSCs) ($CD33^{+}CD11b^{+}HLA\text{-}DR^{-/low}CD15^{-}CD14^{+}$) was identified using the following fluorochrome-conjugated anti-human monoclonal antibodies: anti-CD14 PE-Cy7 (eBioscience), anti-HLA-DR APC (eBioscience), anti-CD15 eFluor® (eBioscience), anti-CD33 FITC (eBioscience), anti-CD11b PE (Beckman Coulter). For each patient, two 5 ml polystyrene round-bottom tubes (BD Falcon) were prepared: 1) a negative control tube with unstained cells (unstained) and 2) a tube

with stained cells (stained). Cells ($5x10^5$) were placed in each tube and incubated with 1X D-PBS (unstained sample) or stained with the appropriate volumes of the labelled multicolour fluorescence anti-human monoclonal antibodies, as reported in **Tables 2** and **3**, and incubated for 20 minutes at room temperature in the dark.

Table 2: Fluorescent anti-human monoclonal antibodies for surface staining of M-MDSCs

Antibody	Unstained	Stained
Anti-Human CD14 PE-Cy7	-	+
Anti-Human HLA-DR APC	-	+
Anti-Human CD15 eFluor®	-	+
Anti-Human CD33 FITC	-	+
Anti-Human CD11b PE	-	+

Table 3: Volumes of fluorescent anti-human monoclonal antibodies used for surface staining of M-MDSCs

Antibody	Volume (µl)
Anti-Human CD14 PE-Cy7	5
Anti-Human HLA-DR APC	4
Anti-Human CD15 eFluor®	4
Anti-Human CD33 FITC	5
Anti-Human CD11b PE	3

Cells were then washed with 2 ml of 1X D-PBS containing 2% FBS, centrifuged at 1500 rpm for 5 minutes, resuspended in 300 µl of 1X D-PBS and analysed using the BD LSR II flow cytometer with BD FACSDiva™ software.

3.6.2 Arginase I expression

MDSCs express high levels of arginase I, an enzyme able to inhibit T-cell function. To confirm the presence/functionality of M-MDSCs in the cell suspensions a flow cytometry-based assay for arginase I expression was performed on selected samples using the Life Technologies permeabilization procedure, according to the manufacturer's instructions. Briefly, freshly isolated total leukocytes ($1x10^6$ cells/ml) were stained as described in the previous paragraph. Then, the cells were washed with 1 ml Hank's salt solution (Millipore) containing Ca^{2+}, Mg^{2+}, phenol red and low endotoxin, centrifuged at 1500 rpm for 5 minutes, resuspended with 100 µl of Fix Solution (provided by the kit), and incubated for 15

minutes. Cells were washed again with 1 ml of Hank's salt solution, centrifuged at 1500 rpm and resuspended in 100 µl of Permeabilization Solution 1X (provided by the kit) containing 4 µl of anti-human Arginase I-Alexa 700 fluorochrome-labelled antibody (R&D systems) for the detection of the intracellular protein. Samples were incubated for 20 minutes, washed with Hank's solution, centrifuged at 1500 rpm for 5 minutes, resuspended in 300 µl of 1X D-PBS and analysed by flow cytometry. All procedure were carried out at room temperature and in the dark.

3.6.3 Phenotypic analysis of T cells

To characterize the T cell subsets in the study cohorts, the percentage and phenotype of $CD4^+$ and $CD8^+$ T cells were investigated on frozen PBMCs. The following parameters were assessed: differentiation status (based on CD45RA and CD27 expression), activation status (based on CD38 and HLA-DR expression), exhaustion status (based on PD1 expression) as well as the presence of regulatory T cells (Tregs). Tregs (also known as suppressor T cells) are a specialized subpopulation of T cells ($CD3^+CD4^+CD25^+FoxP3^+$) that act to suppress immune responses.

To identify these cells a flow cytometry-based assay was used, using the ThermoFisher scientific permeabilization procedure, according to the manufacturer's instructions. To this purpose $1x10^6$ PBMC were placed in 5 ml polysterene round-bottom tubes and stained for 20 minutes with anti-CD4 APC (eBioscience), anti-CD3 BV605 (eBioscience), anti-CD8 APC-Cy7 (BD-biosciences), anti-HLA-DR PE-Cy7 (BD-biosciences), anti-CD38 PE-CF594 (BD-biosciences), anti-PD1 PerCP-Cy5.5 (BioLegend), anti-CD27 Alexa Fluor 700 (BioLegend) and anti-CD45RA V450 (BD-biosciences). Samples were and then washed with 2 ml of 1X D-PBS containing 2% FBS, incubated with 1 mL of Foxp3 Fixation/Permeabilization working solution for 30 minutes, mixed with 2 ml of 1X Permeabilization Buffer, centrifuged at 1500 rpm for 5 minutes, and incubated with the anti-FoxP3 FITC for further 30 minutes. After two final washings with 2 ml of 1X Permeabilization Buffer, the stained cells were resuspended in 300 µl of 1X D-PBS and analysed by flow cytometry. All procedures were carried out at room temperature and in the dark.

3.7 Data processing

Data from flow cytometry were analyzed using the FlowJo VX. 0.7 software. For identification of the M-MDSCs subset, the first gate was placed on PBMCs fraction in FSC and SSC, the second gate on $CD14^+$-HLA-$DR^{-/low}$-$CD15^-$, and finally on $CD33^+$-$CD11b^+$. The monocyte subset (M-MDSCs) corresponds to $CD33^+CD11b^+CD14^+CD15^-$HLA-$DR^{-/low}$ positive cells. Regarding the arginase I

assay, I used the same gating strategy, and added another gate on Arg I^+-SSC to assess the expression of the enzyme in the subset. The percentage of the cells was calculated to the PBMCs gate.

For the characterization of T cells, $CD4^+$ and $CD8^+$ subsets were considered those that were contained in the morphological gate identifying lymphocytes according to FSC and SSC, were positive for CD3 and for CD4 or CD8, respectively. Regarding the differentiation status, naïve T cells were those positive for both CD45RA and CD27. Activated T cells were considered those positive for CD38 and HLA-DR, and exhausted T cells those positive for PD1. Tregs cells were those that, within the CD4 subset, were positive for both CD25 and FoxP3.

3.8 T cell suppression assays

M-MDSCs ($CD33^+CD11b^+CD14^+CD15^-HLA\text{-}DR^{-/low}$) were sorted from $1x10^7$ cells of frozen PBMCs of HCV-infected patients with FACSAria II cell sorter (BD) at the Pediatric Oncoematology Unit of the Azienda Ospedaliera of Padua. Heterologous PBMCs, from healthy donors, were labeled with a solution containing 5 µM 5(6)-carboxy-fluorescein diacetate succinimidyl ester (CFSE, eBioscience) for 10 minutes at 37°C and washed twice before culturing. Labelled PBMCs seeded in 384-well plates (Falcon) coated with 80 µl of anti- human CD3 monoclonal antibody (eBioscience) at 1 µg/ml and cultured without and with sorted M-MDSCs at 2:1 ratio. T cell proliferation was induced by soluble anti-human CD28 monoclonal antibody (Miltenyi Biotec) at concentration of 0,1 µg/ml for 4 days at 37°C. Detached cells were transferred into FASC tubes, washed with 1X D-PBS, centrifuged at 1600 rpm for 5 minutes, and stained with 1 µl of APC-Cy7 anti-human CD8 monoclonal antibody. After vortexing and incubation in the dark at room temperature for 15 minutes, cells were washed with 1 ml of 1X D-PBS at 1600 rpm for 5 minutes, resuspended in 200 µl of 1X D-PBS and analysed by flow cytometry.

3.9 Metabolic Assays

All metabolic assays were performed using frozen PBMCs from selected HCV-infected patients and healthy donors.

3.9.1 ROS production

ROS production in M-MDSCs was detected using the CellROX® Green Reagent (Life Technologies), according to the manufacturer's instructions. To this purpose PBMCs ($1x10^5$) were placed in 5 ml polysterene round-bottom tubes and incubated with the CellROX® Reagent, previously resuspended in DMSO at a

final concentration of 5 μM for 30 minutes at 37°C. Then, the cells were washed twice with 1X D-PBS, centrifuged at 1500 rpm for 5 minutes, and stained for 20 minutes at room temperature in the dark with the specific fluorochrome-conjugated monoclonal antibodies for M-MDSCs identification: anti-human CD15 eFluor450 (eBioscience), anti-human CD33 Alexa Fluor700 (eBioscience), anti-human HLA-DR APC (eBioscience), anti-human CD14 PE-Cy7 (eBioscience) and anti-human CD11b Viogreen ™ (Myltenyi Biotec) (**Table 4**). After a final wash with 1X D-PBS, the stained cells were resuspended in 300 μl of 1X D-PBS and analysed by flow cytometry.

Table 4: Volumes of fluorescent anti-human monoclonal antibodies used for surface staining of M-MDSCs

Antibody	Volume (μl)
Anti-Human CD15 eFluor®	4
Anti-Human HLA-DR APC	4
Anti-Human CD14 PE-Cy7	4
Anti-Human CD33 Alexa Fluor700	5
Anti-Human CD11b Viogreen (TM)	1,5

3.9.2 Mitochondrial membrane potential

Mitochondrial membrane potential in M-MDSCs was measured using the tetramethylrhodamine (TMRM) kit (Life Technologies), according to the manufacturer's instructions. To this purpose PBMCs ($5x10^5$) were placed in 5 ml polysterene round-bottom tubes, and incubated with the tetramethylrhodamine, methyl ester, perchlorate (TMRM) reagent, previously resuspended in DMSO at final concentration of 20 mM, for 30 minutes at 37°C. Then, the cells were washed with cold 1X D-PBS, centrifuged at 1500 rpm for 5 minutes, and stained for 30 minutes at 4°C in the dark with the specific fluorochrome-conjugated monoclonal antibodies, as described in section "Phenotypic analysis of M-MDSCs". After a final wash, with cold 1X D-PBS, the stained cells were resuspended in 300 μl of 1X D-PBS and kept on ice until reading by flow cytometry.

3.10 Analysis of cytokine production

Plasma samples of selected HCV-infected patients and healthy controls were used for the simultaneous quantification of 13 cytokines (GM-CSF, IFNγ, IL-1β, IL-2, IL-4, IL-5, IL-6, IL-7, IL-8, IL-10, IL-12 (p70), IL-13, and TNFα) with Millipore's MILLIPLEX® MAP Human High Sensitivity T Cell Magnetic Bead Panel (Millipore), according to the manufacturer's instructions. The test was

performed with the Bio-Plex 200 System (BioRad) and the Bio-Plex Pro Wash Station (BioRad). The data were analyzed with the software Bio-Plex Manager (BioRad). Briefly, a 96 well plate was shaked with 200 µl of wash buffer supplied by the kit, for 10 minutes at room temperature. After removing the buffer residues, 50 µl of the appropriated standard control and 25 µl of samples were added to the corresponding wells together with 25 µl/well of the mixed beads labelled with the specific antibodies. The plate was wraped with alumin foil and incubated under stirring overnight at 4°C. After incubation the plate was washed 3 times with the wash buffer. Then, 50 µl of detection antibodies were added to each well and the plate further incubated of 1 hour at room temperature under shaking. Immuno-complexes were detected following addition of 50 µl/well of Streptavidin-Phycoerytrhin, incubation for 30 minutes at room temperature, 3 washes and final addition of 150 µl/well of sheath fluid. The plate was finally read with Bio-Plex 200 System (BioRad) and Bio-Plex Manager software presents data as median fluorescence intensity (MFI) as well as concentration (pg/ml).

3.11 RNA extraction from plasma

Plasma samples of 45 selected HCV-infected patients (untreated, under therapy, pharmacologically cured and spontaneously cured) and of 5 healthy donors were used for RNA extraction to analyse the levels of selected miRNAs. The groups of HCV-infected patients chosen for the RNA extraction from plasma are reported in **Table 5**.

Table 5: HCV-infected patients selected for miRNA analysis

Group	Patients (n)
Untreated (NT)	6
Under IFN-free therapy (T) (Ombitasvir+Ritonavir+Paritaprevir+Dasabuvir+Ribavirin)	10
Under IFN-based therapy (T) (PEG-interferon+Telaprevir+Ribavirin)	3
Under IFN-free therapy (T) (Sofosbuvir+Ribavirin)	5
Pharmacologically cured (PC) (Ombitasvir+Ritonavir+Paritaprevir+Dasabuvir+Ribavirin)	10
Pharmacologically cured (PC) (PEG-interferon+Telaprevir+Ribavirin)	3
Pharmacologically cured (PC) (Sofosbuvir+Ribavirin)	5
Relapser (*) (Sofosbuvir+Ribavirin)	1
Spontenously cured	2
Healthy donors	5

(*): Relapser: one patient showed a pick of viremia at 3 month after the end of pharmaceutical treatment.

Prior to RNA extraction, to ensure that plasma samples were not haemolysed, thawed plasma were analysed using a Nanodrop spectrophotometer

(Thermo Scientific) at 200-700 nm wavelength. The presence of a peak at 414 nm indicates presence of lysed red blood cells that may affect the miRNA profile. All selected samples were not haemolysed. Total RNA was extracted from 500 µl of frozen plasma using the miRCURY™ Isolation kit (Exiqon) following the manufacturer's instructions. The samples were centrifuged in a bench centrifuge at 3000 rpm for 5 minutes to pellet any debris and insoluble components. The supernatant (200 µl) of each sample was transferred into a new tube in the presence of 60 µl of lysis solution BF (provided by the kit) and 1,25 µl of MS2 RNA carrier (Sigma-Aldrich). Each tube was vortexed for 5 seconds and incubated for 3 minutes at room temperature. After incubation, 20 µl of Protein Precipitation Solution BF (provided by the kit) was added to each sample which was vortexed for 5 seconds and incubated for 1 minute at room temperature. Each tube was then centrifuged for 3 minutes at 11.000 rpm in a microfuge and the supernatant was transferred in a 2 ml tube. In order to adjust binding conditions, 270 µl of isopropanol were added to the tube and vortexed for 5 seconds. The resulting solution was then loaded onto a miRNA Mini Spin Column BF for RNA purification, according to manufacturer's instructions, and incubated for 2 minutes at room temperature. Each tube was centrifuged for 30 seconds at 11.000 rpm and the flow-through was discarded. The wash and dry procedure began with addition of 100 µl Wash Solution 1 BF (provided by the kit) to the microRNA spin column BF which was centrifuged for 30 seconds at 11.000 rpm. Once discarded the flow-through, 700 µl of Wash Solution 2 BF (provided by the kit) were added to each microRNA spin column BF with a further centrifugation for 2 minutes at 11.000 rpm. This step was repeated by further adding 250 µl of Wash Solution 2 BF and centrifuging for 1 minutes at 11.000 rpm to dry the membrane completely. Each microRNA spin column BF was placed in a new 1.5 ml tube incubated with 50 µl RNase free H_2O to elute the purified small RNA. The subsequent incubation was followed by centrifugation for 1 minute at 11.000 rpm. Finally, RNA samples were stored at -20°C and, the following day, they were moved at - 80°C until use.

3.12 MicroRNA qRT-PCR service

The total RNA extracted using miRCURY™ Isolation kit were shipped on dry ice to Exiqon (Denmark), which provided the service for RNA quality and microRNA qPCR as well as comprehensive analysis. Briefly, each RNA was reverse transcribed into cDNA and run on the miRCURY LNA™ Universal RT miRNA PCR Human panel I and II (Exiqon) in order to detect the levels of four selected circulating microRNAs: miRNA-122-5p, miRNA-196b-5p, miRNA-21-5p, miRNA-29a-3p. In addition, UniSp6 (RNA-Spike in oligonucleotide) was added to each reaction as internal control for cDNA synthesis.

miRNA-122 and miRNA-21 have been chosen because several studies reported their presence in patients with chronic HCV infection and their stimulatory role in HCV replication (Dian X. et al., 2013; Xu J. et al., 2011). In contrast, miRNA-196b and miRNA-29a inhibit the HCV replication process (Hoffmann T.W. et al., 2012). Furthermore, miRNA-29a, miRNA-21 and miRNA-196b seem to participate in myeloid progenitor expansion (Tian J. et al., 2014).

The amplification of cDNA was performed using a LightCycler 480 Real-Time PCR System (Roche) using the SYBR^{TM} Green master mix (Exiqon). Each miRNA was assayed twice and each amplification product was subject to quality control. The amplification curves were analysed using the Roche LC software, both for determination of Ct (threshold cycle) by the second derivate method and for melting curve analysis. The efficiency was calculated using algorithms similar to the LinReg software, where the efficiencies range between 1,8 and 2,1. The individual reactions with amplification efficiency below 1,6 value were excluded. All assays were inspected for distinct melting curves and the Tm was checked to be within known specifications for the assay. Furthermore, to be included in the data analysis, each sample assay data point must be detected with 5 Cts less than the negative control assay data point, and with a Ct < 37. Data that did not pass these criteria were excluded from any further analysis. Since miRNA-103a is very stable in human plasma, all data were normalized using miRNA-103a as internal reference to correct for potential overall differences between the samples.

3.13 Statistical analysis

All data regarding the M-MDSCs were analysed by using the GrafhPad Software 6.0 statistical analysis. Quantitative data normally distributed were expressed as mean ± standard deviation (SD), followed by independent *t*-test used to compare the difference of mean between two groups. For normally distributed data, variables were expressed as medians and nonparametric Mann-Whitney test were used to compare the difference of median between two groups. The one-way analysis of variance (ANOVA) was used to determine any statistically significant differences between the means of three independent (unrelated) groups, Bonferroni correction was used. The correlation between the frequency of M-MDSC and patients clinical parameters was analysed by Spearman's rank test, and a *P* value less than 0,05 was considered to be statistically significant. miRNAs expression was analyzed with a Shapiro-Wilk test for check if the data were normally distributed, nonparametric Wilcoxon test and chi-squared test were used to compare the difference between two groups and *P* value less than 0,05 was considered to be statistically significant, Benjamini-Hochberg correction for multiple testing was used.

4. RESULTS

4.1 Study groups

HCV-chronically infected patients (n=262) were enrolled for this study (**Figure 9**) and grouped in: 1) untreated patients (n=75) (NT, no therapy); 2) patients during pharmacological treatment (n=70) (T, therapy); 3) patients with cleared infection after pharmacological therapy (n=115) (PC, pharmacologically cured), including patients treated with IFN-based therapies (T, n=10, and PC, n=38) and with IFN-free therapies (only DAAs) (T, n=60.; PC, n=77) and 4) patients who have spontaneously cleared HCV infection (n=2) (SC, spontaneously cured). In addition, 47 donors were enrolled as healthy controls (HC). The baseline characteristics of the enrolled participants are summarized in **Table 6**.

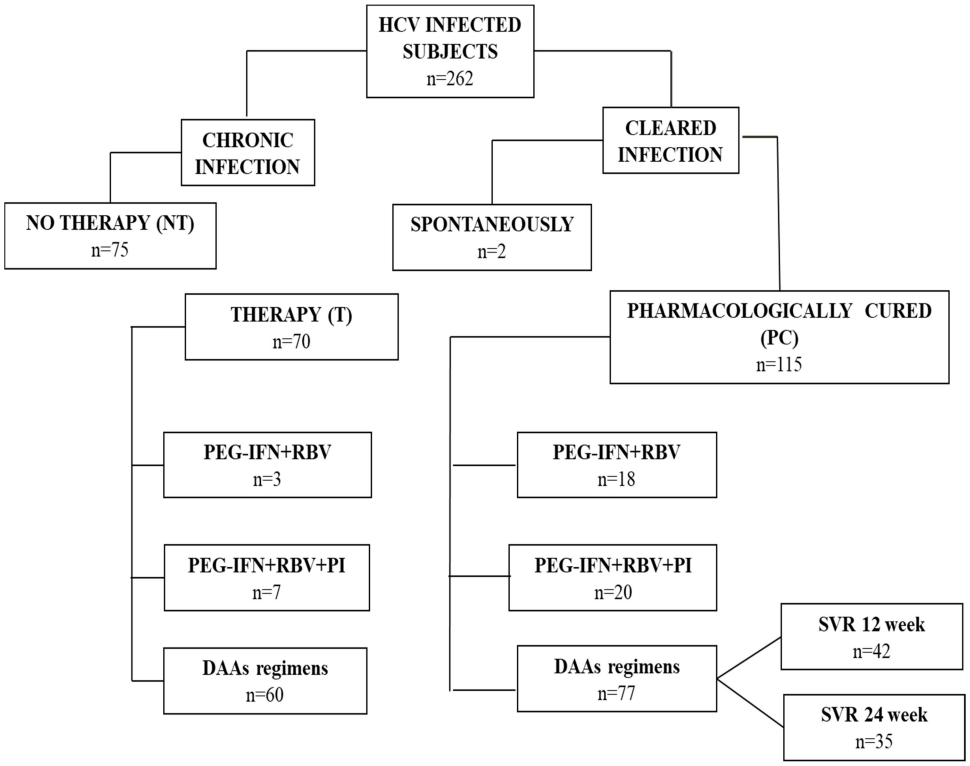

Figure 9: Study groups. RBV, ribavirin; PEG-IFN, PEGylated interferon; PI, protease inhibitor; DAAs, direct acting antiviral agents; SVR, sustained virologic response

Table 6: Basic characteristics of HCV-infected volunteers

HCV-infected patients			
Index	**[a]NT**	**[b]T**	**[c]PC**
Total subjects (n)	75	70	115
Sex (n) (male/female)	35/40	36/34	59/56
Age (n) (<50/>50)	23/52	17/53	33/82
HCV genotype (n)	1 (43)	1 (44)	1 (86)
	2 (8)	2 (10)	2 (14)
	3 (15)	3 (12)	3 (7)
	4 (9)	4 (4)	4 (7)
	5 (0)	5 (0)	5 (1)
HCV RNA IU/mL (range)	$2{,}01x10^6$ ($3{,}8$-$2{,}77x10^7$)	54,97 (0-990)	0
AST U/L (range)	63,62 (12-374)	35,09 (17-144)	25,32(13-50)
ALT U/L (range)	78,7 (10-587)	33,01 (10-147)	21,70 (10-40)
Leucocyte cell/mL (mean)			
IFN-based therapy	$1{,}19x10^3$	$0{,}80x10^3$	$1{,}12x10^3$
IFN-free therapy		$1{,}37\ x10^3$	$1{,}15x10^3$

[a]NT, not treated; [b]T, in therapy; [c]PC, pharmacologically cured

4.2 Phenotypic characterization of monocytic myeloid derived suppressor cells (M-MDSCs): surface markers and arginase I expression

I have focused my attention on monocytic MDSCs (M-MDSCs) because, as other reports already showed, is the most abundant MDSCs population in patients infected by HCV.

The gating strategy was standardized according to Nonnenmann J. et al. (2014), as detailed in the Materials and Methods section. A clear population of M-MDSCs ($CD33^+CD11b^+HLA\text{-}DR^{-/low}CD14^+CD15^-$) was displayed in the samples analysed, as shown in **Figure 10**.

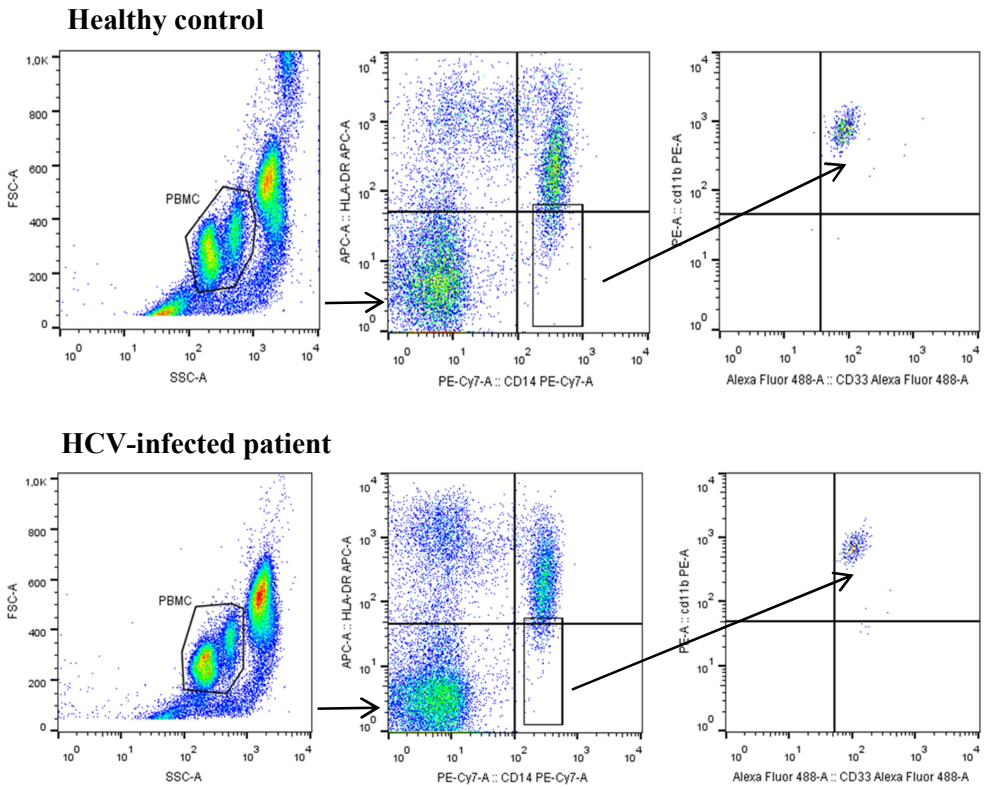

Figure 10: Representative dot plots and gating strategies for the M-MDSCs subset. The gates are set on $CD33^{+}CD11b^{+}HLA\text{-}DR^{-/low}CD14^{+}$ cells populations. The top panel shows one representative healthy control and the bottom panel one representative HCV-chronically infected patient.

Since the expression of Arginase I is a functional feature common to M-MDSCs (Gabrilovich D.I. and Nagaraj S., 2009), to confirm that the gated cells are MDSCs, a flow cytometry-based assay for arginase I expression was then performed. As shown in **Figure 11**, M-MDSCs express this enzyme, confirming that the selected gating strategy allows a proper identification of the M-MDSC subset.

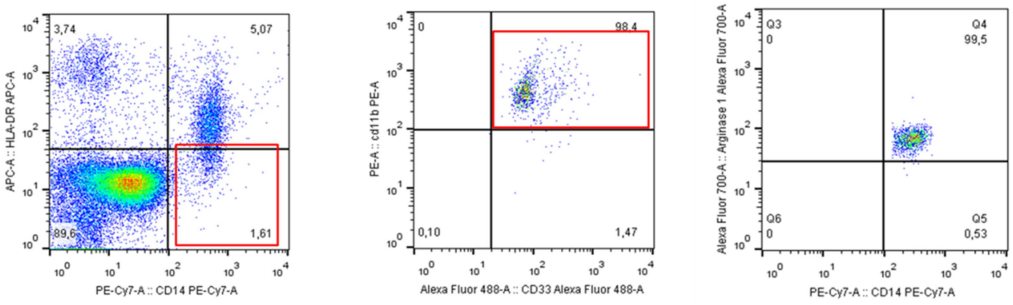

Figure 11: Gating strategy for the analysis of arginase I expression with the gating strategy for M-MDSC. One representative sample is shown.

4.3 The frequency of M-MDSCs in all patients with HCV-chronic infection is higher than in healthy controls irrespective of the presence (and the type) or absence of therapy

The frequency of M-MDSCs was then analysed in peripheral blood of patients with HCV-chronic infection without therapy (NT), during therapy (T), pharmacologically cured (PC) and of healthy controls (HC). Overall, a significantly higher number of M-MDSCs was detected in all HCV-infected patients (irrespective to their status NT, T or PC and of the type of therapy) compared to healthy controls (HC) ($p<0,0001$). In fact, as shown in **Figure 12**, the mean percentage values (±SD) of the M-MDSCs in the NT, T, PC and HC groups were 3,71 (±2,98), 3,15 (±2,7), 2,06 (±1,19) and 1,04 (±0,55), respectively.

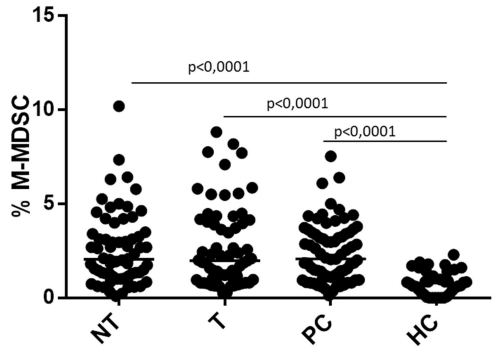

Figure 12: Frequency of M-MDSCs in HCV-chronically infected patients not treated (NT) (n=66), during therapy (T) (n= 63), and pharmacologically cured (PC) (n= 74) compared to healthy controls (HC) (n=38). [*Mann-Whitney test*]

These results are in agreement with previous studies reporting higher levels of M-MDSCs in untreated HCV-infected patients as compared to healthy controls (Tacke R.S. et al., 2012; Cai W. et al., 2013) and apparently suggest that HCV antiviral treatments do not exert any specific effect on this subset of immune-regulatory cells.

However, to evaluate whether the presence of IFN-based and IFN-free antiviral therapies may be associated to immunomodulatory effects and restoration of immune functions, the levels of M-MDSCs were compared among patients under therapy (T) and patients pharmacologically cured (PC) stratified by type of therapy. In particular, three T and PC groups, including 1) Peg-IFN+RBV, 2) Peg-IFN+RBV+PI and 3) DAAs (IFN-free therapies) were compared to HC.

As shown in **Figure 13A**, during DAA therapies the mean percentage of M-MDSCs (3 ±2,18) was significantly higher ($p<0,0001$) as compared to healthy controls (1,04 ±0,55). In addition, under DAA therapies, the mean percentages of

M-MDSCs (3 ±2,18%) were overall higher as compared to M-MDSCs (Peg-IFN+RBV: 0,96 ±0,39; Peg-IFN+RBV+PI: 1,97 ±2,6) during IFN-based treatments (p=0,037), although I cannot exclude that this difference maybe due to the limited number of the patients being treated with IFN-based regimens.

As shown in **Figure 13B**, after viral clearance, the mean numbers of M-MDSCs were comparable (p>0,05) in the PC groups (Peg-IFN+RBV: 2,01 ±1,27; Peg-IFN+RBV+PI: 2,69 ±1,58; DAAs: 2,44 ±1,66) and overall still significantly higher compared to healthy controls (p<0,0001).

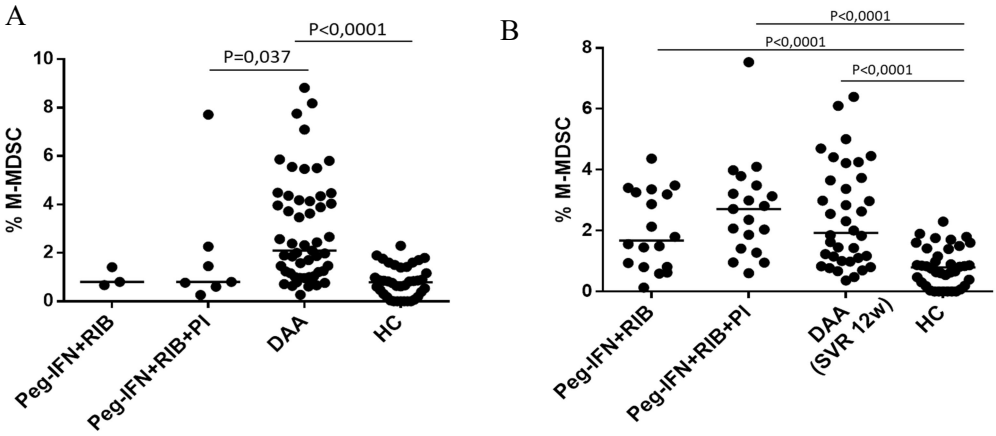

Figure 13: Frequency of M-MDSCs in HCV-chronically infected patients under different antiviral therapies (T) (panel A) and pharmacologically cured (PC) (panel B). (A) Peg-IFN+RBV (n=3), Peg-IFN+RBV+PI (n=7) and DAA (n=53). (B) Peg-IFN+RBV (n=18), Peg-IFN+RBV+PI (n=20) and DAA (SVR 12week) (n=35). All patients were compared with HC (n=38). [*Ordinary One-Way* and *Mann-Whitney test*]

The results of these analyses indicate that the percentages of M-MDSCs, in IFN-based or IFN-free groups, are similar (both during the therapy and after viral clearance at the end of the therapeutic protocol) and comparable to those of NT patients. Specifically for DAA-based therapies this comparison was performed at week 12 after the end of treatment (SVR 12week). Taken together, these data suggest that both types of HCV antiviral therapies (IFN-based and IFN-free) do not restore the frequency of M-MDSCs to the levels of healthy controls. For DAAs therapy this is true at least at SVR12week.

4.4 The increase of M-MDSCs during HCV-chronic infection does not correlate with the patients' features (stage of liver diseases, age, sex, clinical parameters) nor with the presence of specific viral genotypes

The stage of the liver disease can be classified using several scales, but the most common is classification from F1 to F4 [mild liver fibrosis (F1), moderate

fibrosis (F2), severe fibrosis (F3) and cirrhosis (F4)], as established by liver biopsy whose results were made available to us (**Table 7**).

Table 7: Stage of liver disease

HCV-chronically infected patients			
Index of fibrosis	**[a]NT** (n)	**[b]T** (n)	**[c]PC** (n)
F1	40	11	31
F2	6	3	8
F3	8	9	6
F4	12	40	29

[a]NT, not treated; [b]T, during therapy; [c]PC, pharmacologically cured

For each stage of liver disease, I have analysed the frequencies of M-MDSCs in order to understand if there is any correlation between the progression and the healing of disease. The frequency of M-MDSCs in NT and PC cohorts, stratified by kind of therapy, was compared (**Figure 14)**.

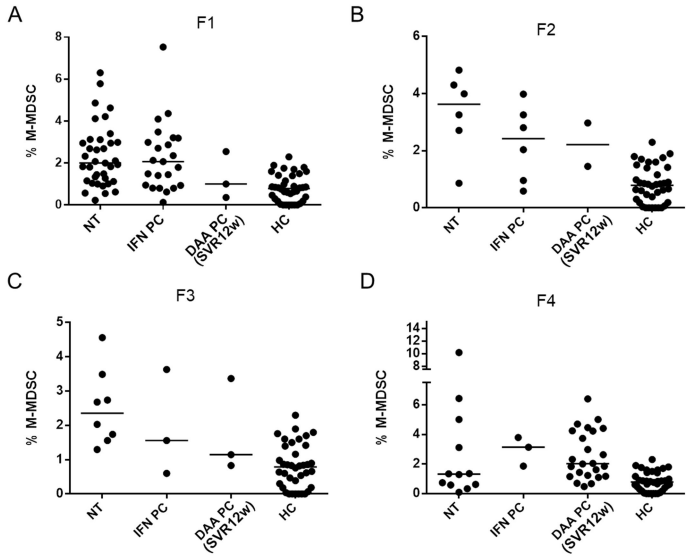

Figure 14: Percentages of M-MDSCs in in patients not in therapy (NT), and pharmacologically cured (PC) at SVR 12week, with interferon-based therapy (IFN PC) and with DAA regimens (DAA PC). [*Ordinary One-Way* and *Mann-Whitney test*]

The results showed no significant differences between the percentages of M-MDSCs in NT and PC patients, stratified by liver disease stage. These results are in agreement with the study of Nonnenmann J et al. (2014).

In **Figure 15**, HCV-infected patients (NT, T, PC) were analysed according to their age (< or > 50 years). The percentages of M-MDSCs were comparable

(p>0,05) among NT, T and PC groups and were not influenced by the age. In contrast with our results, previous studies have found a positive correlation between increased levels of MDSCs and the older age of the patients during HCV infection (Ning G. et al., 2015). A possible explanation could be that they analyzed a smaller number of patients.

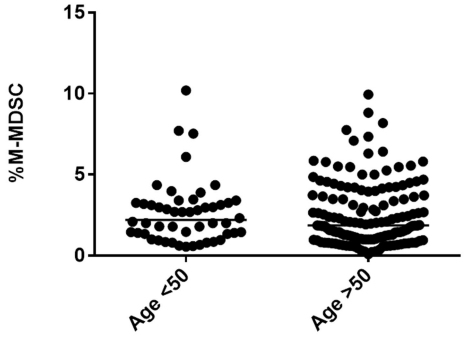

Figure 15: Frequency of M-MDSCs according to age, < 50 years (left panel) (n=47) or >50 years (right panel) (n=144). [*Ordinary One-Way* and *Mann-Whitney test*]

When I analysed the percentages of M-MDSCs according to the sex of HCV-infected patients: in contrast with previous observations (Liu Y. et al., 2014) demonstrating higher frequencies of M-MDSCs in males, I observed comparable frequencies of M-MDSC between males and females (p>0,05) (**Figure 16**). This contrasting result is maybe due to the fact that I have analyzed a larger cohort of patients.

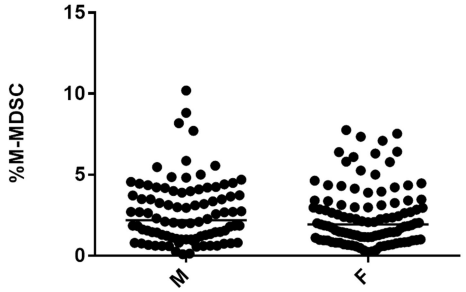

Figure 16: Percentages of M-MDSCs depending on the sex of patients: female (F) (n=93) and male (M) (n=105). [*Mann-Whitney test*]

Finally, I have evaluated the correlation between M-MDSC levels and some prognostic markers, including HCV viral load and liver enzymes (see **Table 6**). The results showed no significant correlation in the frequencies of M-MDSCs with the HCV RNA load (p>0,05) (**Figure 17**), alanine transaminase (ALT) or aspartate transaminase (AST) levels (**Figures 18 and 19**).

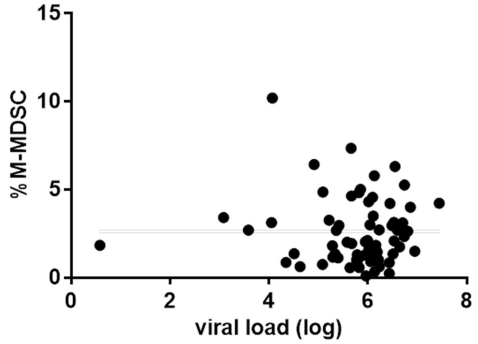

Figure 17: Correlation analysis between M-MDSCs and viral loads in HCV-infected patients not treated (n=66). [*Linear regression*]

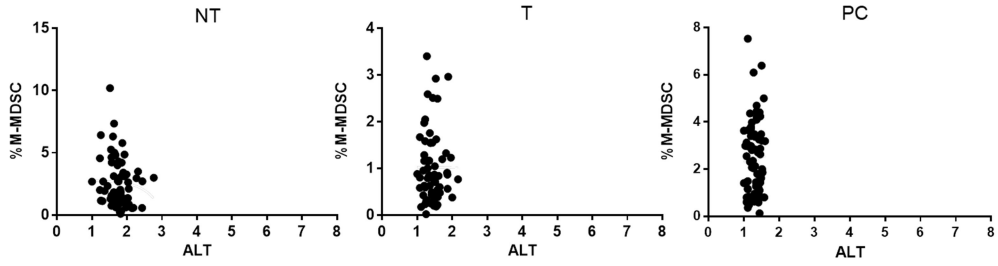

Figure 18: Correlation between M-MDSCs and serum ALT levels in patients untreated (NT, n=66), under therapy (T, n=63) and pharmacologically cured (PC, n=74) patients. [*Linear regression*]

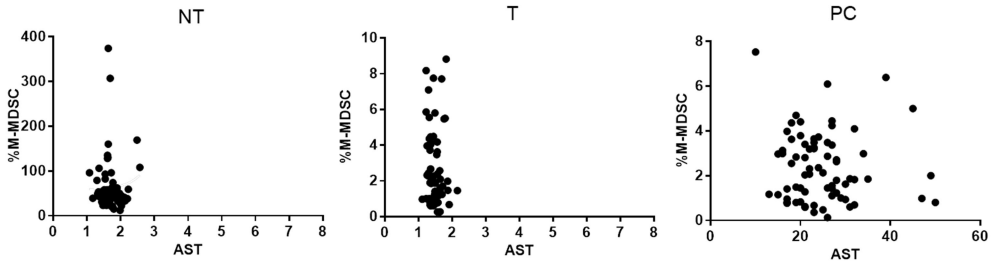

Figure 19: Correlation between M-MDSCs and serum ALT levels in patients untreated (NT, n=66), under therapy (T, n=63) and pharmacologically cured (PC, n=74) patients. [*Linear regression*]

Eventually I have evaluated whether the presence of a specific HCV genotype may influence the levels of M-MDSCs. For this purpose I have analyzed the frequencies of these cells in groups of patients infected with the same genotype. The genotypes 1, 2, 3 and 4 were the most common in patients enrolled in this study with a prevalence of genotype 1 (see **Table 6**). In general, the proportion of MDSCs did not correlate, with the presence of a specific HCV genotype (**Figure**

20), as also shown in previous studies (Liu Y. et al., 2014; Nonnenmann J. et al., 2014).

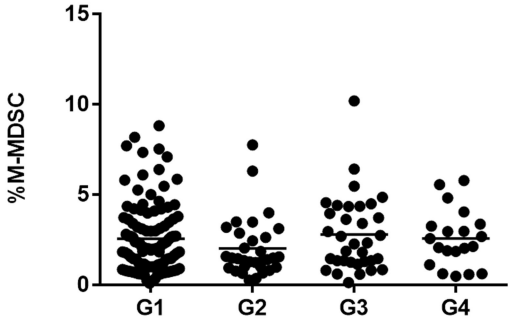

Figure 20: Percentages of M-MDSCs respect to HCV genotypes (G) 1, 2, 3 and 4 in patients not in therapy (NT, n=66), in therapy (T, n=63) and pharmacologically cured (PC, n=74). [*Ordinary One-Way* and *Mann-Whitney test*]

As patients infected with different HCV genotypes may undergo different DAA-based regimens, next I stratified the patients by HCV genotype, to assess if DAAs could affect the number of M-MDSCs in patients infected with a specific genotype. However, as shown in the **Figure 21**, for each genotype considered I did not detect any significant difference between NT, T and PC patients.

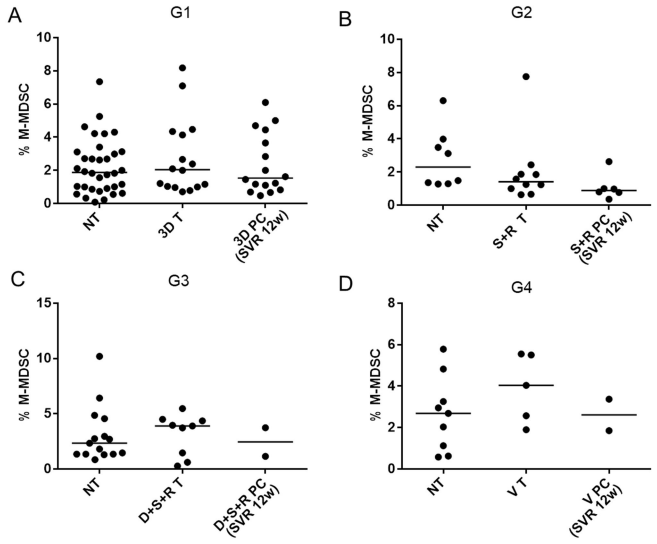

Figure 21: Percentages of M-MDSCs in relation with DAAs treatment and HCV genotypes (G) 1, 2, 3 and 4. (A) 3D Abbvie (NT n=34, T n=16, PC n=16); (B) sofosbuvir + ribavirin (S+R) (NT, n=8; T, n=10, PC, n=6); (C) daclatasvir+sofosbuvir+ribavirin (D+R+R) (NT, n=15; T, n=9; PC, n=2) and (D) Viekirax (V) (NT, n=9; T, n=5; PC, n=2). [*Ordinary One-Way* and *Mann-Whitney test*]

4.5 Comparison between the M-MDSCs frequency during and after the end of therapy with IFN-free drugs

For 22 HCV-infected patients treated with IFN-free therapies we obtained longitudinal blood samples at three time points: during therapy (T), and after viral clearance at 3 and 6 months (PC SVR 12week, and PC SVR 24week). First of all, I compared the frequencies (%) of M-MDSCs between T (3 ±2,18) and PC at SVR 12week (3,09 ±1,63) (**Figure 22**) and, as previously observed, these values were similar between the two groups and higher ($p<0,0001$) than healthy controls (1,04 ±0,55).

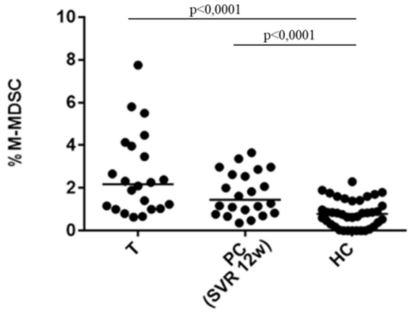

Figure 22: Frequencies of M-MDSCs of 22 selected patients, for whom longitudinal samples were available, during IFN-free therapy (T), after viral clearance SVR 12week (PC) and healthy control (HC, n=38). [*Mann-Whitney test*]

However, as shown in **Figure 23**, after 6 months (SVR 24week) from virus clearance the frequency of M-MDSCs (1,27 ±0.67%) was restored to levels comparable to healthy controls (1,04 ±0,55%) and significantly lower than M-MDSCs counts (3,09 ±1,63%) after 3 months (SVR 12week) ($p<0,0001$). These data suggest that after viral clearance with DAA-based therapies the restoration of M-MDSCs numbers to physiological levels can occurs but it takes time, since it was observed only after 6 months from the end of the therapeutic protocol.

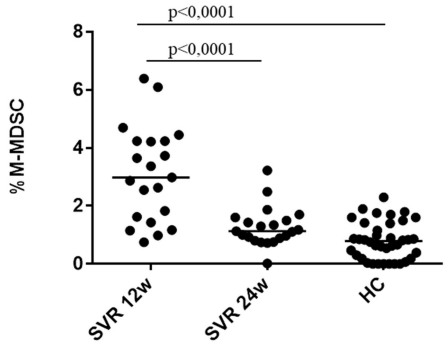

Figure 23: Levels of M-MDSC at SVR 12week and SVR 24week in 22 selected patients for whom longitudinal samples, during therapy and after viral clearance, were available. [*Mann-Whitney test*].

A further evaluation of the data pointed out a correlation between the number of M-MDSC after SVR 12week and their proportional decrease at SVR 24week (**Figure 24**).

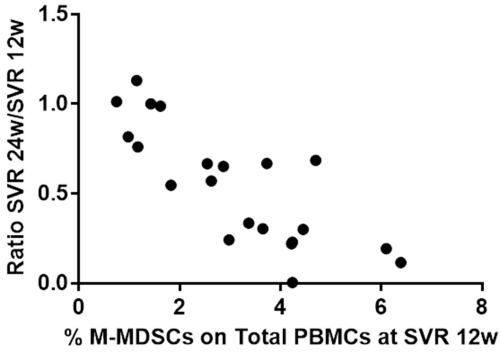

Figure 24: Correlation between frequency of M-MDSCs in DAA-treated patients after SVR 12week and the ratio among the frequency at 24week/12week.

4.6 Cytokines profile

A common denominator in infection and cancer biology is systemic inflammation, with production of mediators like cytokines. For instance, an increase of pro-inflammatory cytokines IL-1beta, IL-6, and TNF-alpha has been associated with HCV infection (Fallahi P. et al., 2012).

To date, for most infections, expansion of M-MDSCs is explained by generation of inflammatory mediators during the course of the disease. In addition, growth factors, such as GM-CSF, foster the generation of M-MDSCs by promoting emergency myelopoiesis, skewing differentiation of progenitors into monocytes and DCs (STAT3/STAT5 activation) and promoting survival of M-MDSCs (Dorhi A. and Du Plessis N., 2018).

Thus, to better understand the decrease of M-MDSC percentages occurring in pharmacological cured patients only 24 weeks after viral clearance, I performed a longitudinal analysis in selected (n=9) plasma samples of these 22 patients collected at 2 time points: at SVR 12week and 24week. The levels of the following 13 cytokines was measured: GM-CSF, IFNγ, IL-1β, IL-2, IL-4, IL-5, IL-6, IL-7, IL-8, IL-10, IL-12 (p70), IL-13, and TNFα. Notably, a significant downregulation of GM-CSF (from a mean value of 50,03 to 40,98 pg/ml) and IL-10 (from a mean value of 32,68 to 24,80 pg/ml) was observed from week 12 to 24. In contrast, we observed a significant, although subtle, increase of TNFα (from a mean value of 6,92 to 8,21 pg/ml) (**Figure 25**).

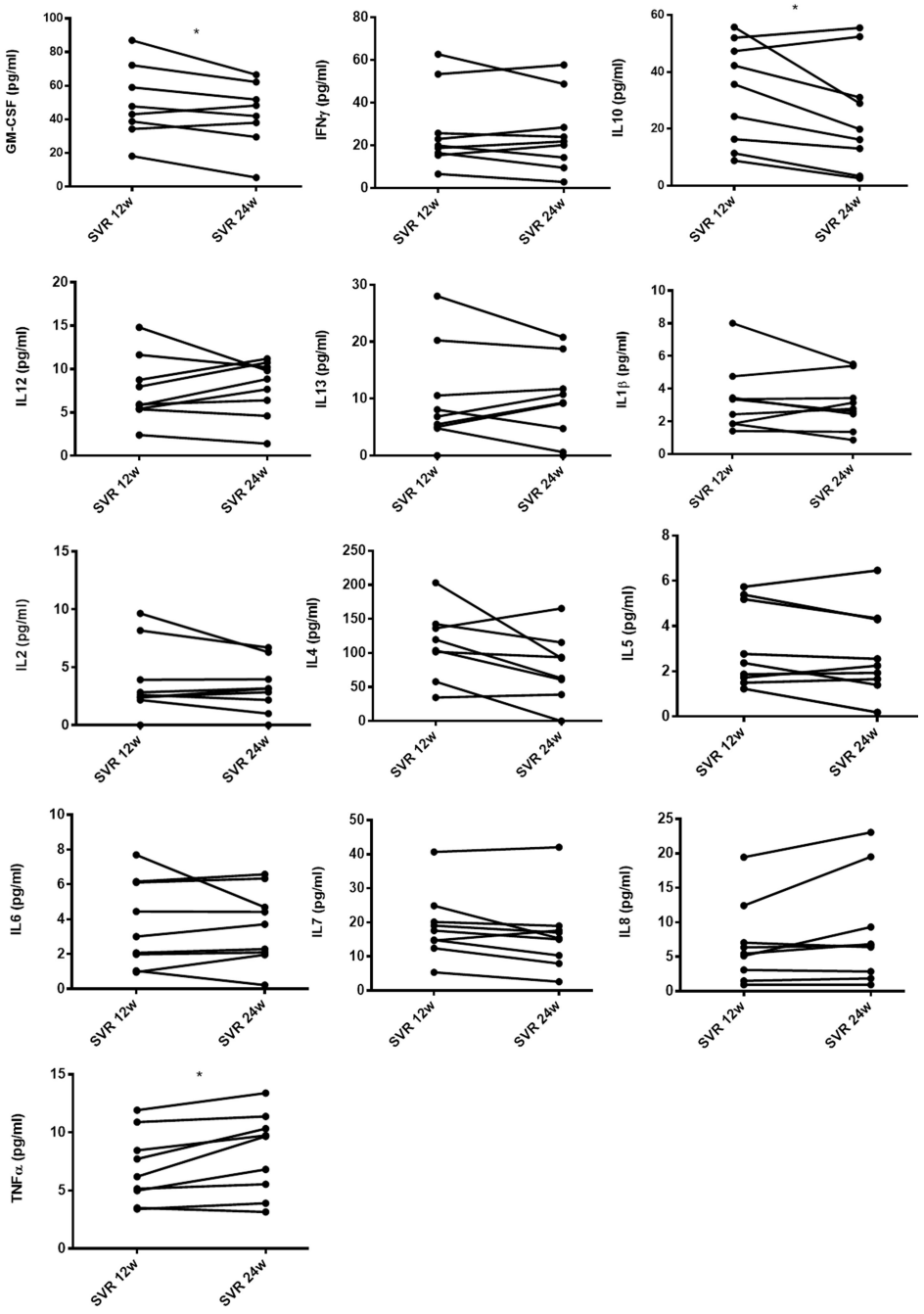

Figure 25: Cytokines levels in in DAA-treated patients at two time points after viral clearance: SVR 12week and SVR 24week (*=p<0,05). [*Wilcoxon signed-rank test*]

It is interesting to note the decrease of GM-CSF and IL-10, both involved in the accumulation and activation of MDSCs; this may explain the decrease of M-MDCS percentages we observed in patients between week 12 and 24 after viral clearance.

4.7 T cell suppression assays

MDSCs are known to suppress immune responses in a variety of ways, depending on the specific pathological conditions. In particular, during chronic viral infections (including HCV infection), MDSCs dampen the immune responses suppressing the functionality and proliferation of T lymphocytes. I thus performed suppression assays to assess the capability of MDSCs from HCV-infected individuals to suppress the expansion of activated $CD8^+$ T cell. To this aim, I cultured for 4 days CFSE-labeled peripheral blood mononuclear cells (PBMCs) from healthy donors (stimulated with anti-human CD3 and anti-human CD28 monoclonal antibodies to induce T cell proliferation) with $CD14^+HLA\text{-}DR^{-/low}CD15^-CD33^+CD11b^+$ (M-MDSCs) cells sorted (by flow cytometry) from HCV-infected patients. As shown in **Figure 26**, while $CD8^+$ T cells activated in the absence MDSCs exhibited a classical profile of proliferation, those activated and cultured in the presence of MDSCs showed a substantial reduction of proliferation (32% reduction in the shown representative example).

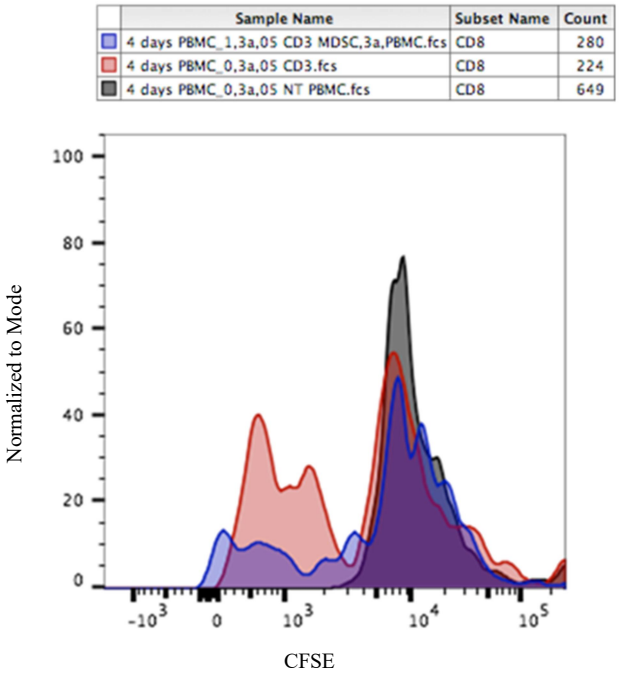

Figure 26: Representative histogram of a T cell suppression assay; in black PBMCs not stimulated, in red PBMCs stimulated with anti-human CD3 and anti-human CD28 monoclonal antibodies and, finally, in blue PBMCs, stimulated with anti-human CD3 and anti-human CD28 monoclonal antibodies, co-cultured with M-MDSCs.

The optimization of the protocol was a laborious process, as the assays is technically challenging. Indeed, the sorting of viable cells and their culturing for a

relative long time period with an heterologous cells population is necessary. In addition, I had to adapt the assay conditions to the low number of MDSCs that can be sorted from frozen PBMCs of HCV-infected patients.

4.8 Phenotypic analysis of T cells

HCV-infection is known to cause a status of systemic chronic immune activation and exhaustion of T cells that is, in part, responsible for the lack of spontaneous viral clearance. To assess if DAAs therapy could restore T cell homeostasis, I analyzed in the different study groups (HC, NT, T, SVR 12week and SVR 24week): the differentiation status (CD45RA and CD27 expression), the activation profile (based on CD38 and HLA-DR expression) and the exhaustion levels (based on PD1 expression) of different T cell subsets.

Subsets of $CD4^+$ and $CD8^+$ T cells were defined by the surface expression of CD45RA and CD27 as: naïve cells (N) $CD45RA^+$-$CD27^+$, central memory cells (CM) $CD45RA^-$-$CD27^+$, effector memory cells (EM) $CD45RA^-$-$CD27^-$ and terminally differentiated effector memory cells (EMRA) $CD45RA^+$-$CD27^-$ (**Figure 27**).

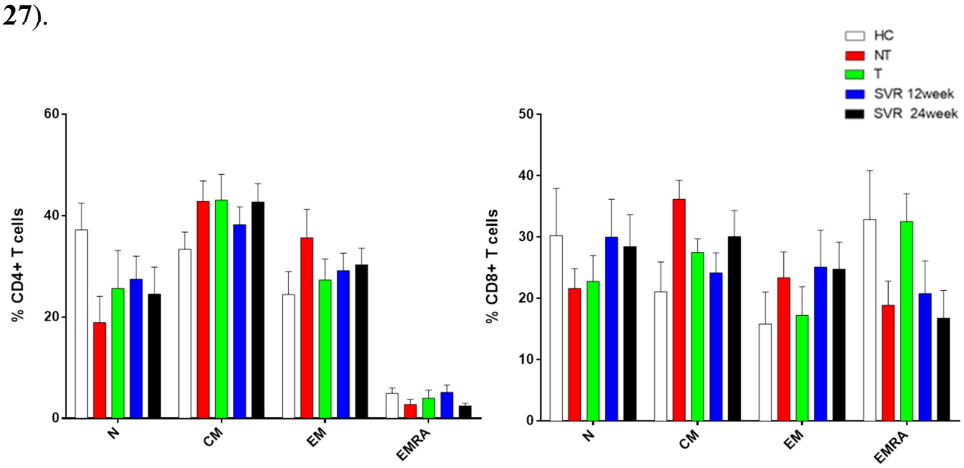

Figure 27: Percentage of different $CD4^+$ (left panel) and $CD8^+$ T (right panel) cells subpopulation: naïve (N), central memory (CM), effector memory (EM) and terminally differentiated effector memory cells (EMRA) in healthy controls (HC, n=10), not treated patients (NT, n=10), treated patients with DAAs therapy (T, n=6), patients pharmacologically cured (after DAAs therapy) after 12 weeks (SVR 12week, n=9) and 24 weeks (SVR 24week, n=11).

HCV infection perturbs the subset distribution among both $CD4^+$ and $CD8^+$ T cell compartments. In particular, it is interesting to note the increase of the both $CD4^+$ and $CD8^+$ CM T cells in NT HCV-infected patients, which is not restored after viral clearance. In addition, HCV infection induced a stable decrease of N $CD4^+$ T cells and EMRA $CD8^+$ T cells, even in treated patients.

Subsequently I evaluated the activation status of CD4 and CD8 subpopulations determined by the co-expression of CD38 and HLA-DR (**Figure 28**).

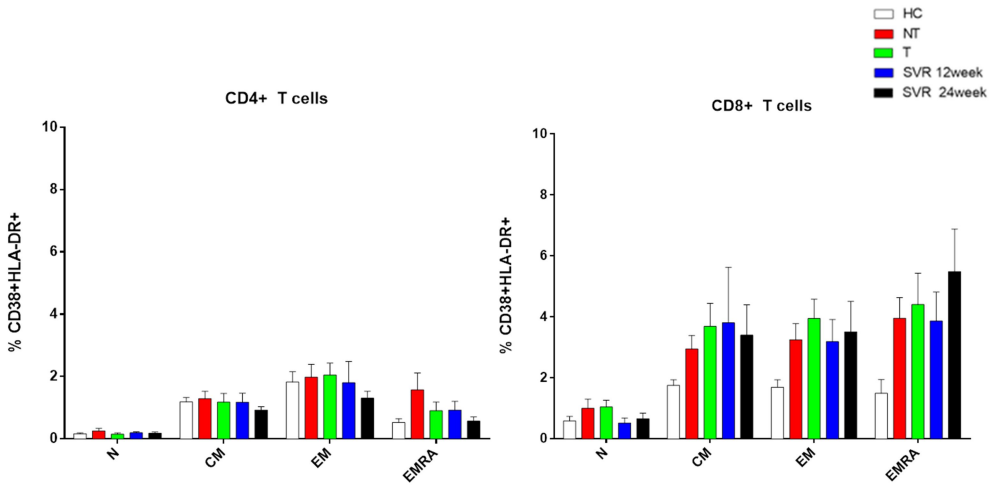

Figure 28: Expression of CD38 and HLA-DR in $CD4^+$ (left panel) and $CD8^+$ (right panel) T cells: naïve (N), central memory (CM), effector memory (EM) and terminally differentiated effector memory cells (EMRA) in healthy controls (HC, n=10), not treated patients (NT, n=10), treated patients with DAAs therapy (T, n=6), patients pharmacologically cured (after DAAs therapy) after 12 weeks (SVR 12week, n=9) and 24 weeks (SVR 24week, n=11).

$CD4^+$ T cell subsets did not show increased levels of activation in HCV-infected patients compared to healthy subjects. In contrast, I noticed in all study groups (NT, T, SVR 12week and SVR 24week) an increased activation of memory $CD8^+$ T cell subsets (CM, EM and EMRA) compared with HC. Interestingly, even 6 months after viral clearance activation levels were still elevated. In contrast, while N $CD8^+$ T cells from NT showed slightly higher activation levels compared to HC, DAAs therapy seems to quickly normalize this phenomenon.

Finally considering that chronic viral infections are frequently characterized by functional impairment of T cells, I focused my attention on the expression of the exhaustion marker PD1. Our data suggest that only CM $CD8^+$ T cells expressed high levels of PD1 in non-treated HCV infection (**Figure 29**), a phenomenon not restored by DAAs therapy as PD1 levels were still elevated at month 6.

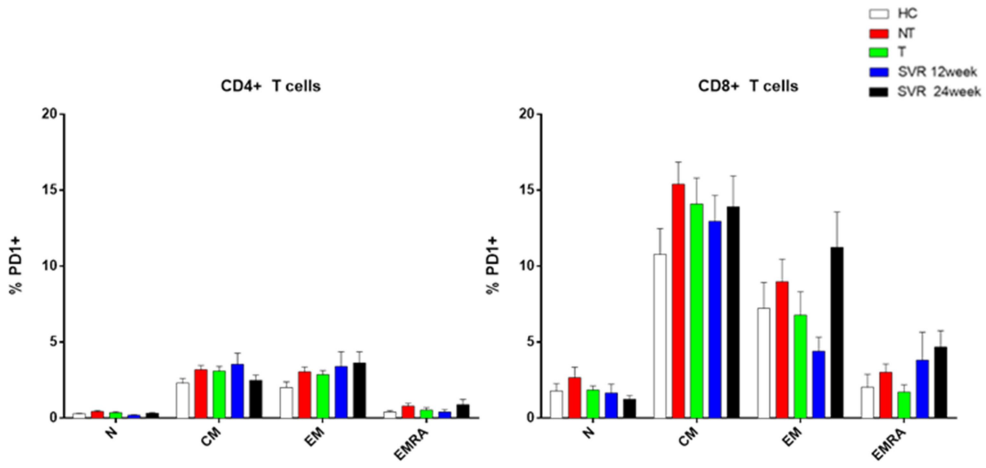

Figure 29: Expression of PD1 in $CD4^+$ (left panel) and $CD8^+$ (right panel) T cells subpopulation: naïve (N), central memory (CM), effector memory (EM) and terminally differentiated effector memory cells (EMRA) in healthy controls (HC, n=10), not treated patients (NT, n=10), patients treated with DAAs therapy (T, n=6), patients pharmacologically cured (after DAAs therapy) after 12weeks (SVR 12week, n=9) and 24weeks (SVR 24week, n=11).

Taken together, these data suggest that the restoration of the T cell compartment is a slow process that may take several months after viral clearance.

Finally, I analyzed the presence of regulatory T cells (Treg) identified as $CD3^+CD4^+CD25^+FoxP3^+$ (**Figure 30**), that studies suggest as one of the major responsible for the dysfunctions of HCV-specific T cells in chronically infected patients (Accapezzato D. et al., 2004; Cabrera R. et al., 2004). Also, it was recently described the ability of MDSCs to promote the *de novo* development of Treg cells *in vivo* (Huang B. et al., 2006). The frequency of circulating Treg in HCV not-treated patients (NT) was significantly higher compared to healthy controls (p=0,049). In addition, a tendency toward higher Treg numbers in all DAA treated HCV-infected individuals compared to healthy controls was observed.

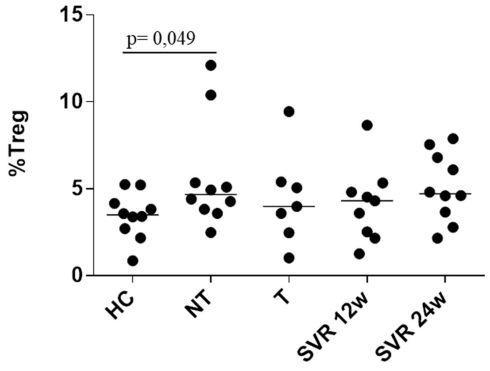

Figure 30: Frequency of regulatory T cells (Tregs) in healthy controls (HC, n=10), not treated patients (NT, n=8), patients treated with DAAs therapy (T, n=6), patients pharmacologically cured (after DAAs therapy) after 12 weeks (SVR 12week, n=8) and 24 weeks (SVR 24week, n=10). [*Mann-Whitney test*]

4.9 Metabolic assays

4.9.1 ROS measurements

As one of the suppression mechanisms used by MDSCs is the overproduction of reactive oxygen species (ROS), I evaluated the ROS production by M-MDSCs expressed as mean fluorescents intensity (MFI) in the different groups of interest (**Figure 31**).

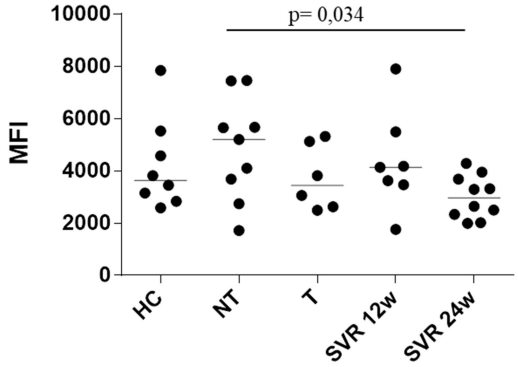

Figure 31: ROS levels in M-MDSC in: healthy controls (HC, n=10), not treated patients (NT, n=9), patients treated with DAAs therapy (T, n=6), patients pharmacologically cured (after DAAs therapy) after 12 weeks (SVR 12week, n=7) and 24 weeks (SVR 24week, n=10). [*Mann-Whitney test*].

Looking at **Figure 31**, a trend towards higher ROS production by M-MDSCs in untreated patients (NT) compared to healthy controls could be observed. Notably, lower levels of ROS in MDSCs were noticed already in patients under treatment (T), and those at SVR 24 week showed a significant decline in ROS

production from MDSCs compared to NT. This could mean that the reduction of ROS production in M-MDSCs, to levels similar to those of healthy controls, is apparent before the complete eradication of the infection already during the intake of DAAs therapy.

4.9.2 Mitochondrial membrane potential

Mitochondrial dysfunctions have been associated with various disorders such as cancer, cardiovascular diseases, diabetes, and neurodegenerative diseases (Pieczenik S.R. and Neustadt J., 2007). In addition, mitochondrial function is a key indicator of cell health. Thus, to measure M-MDSCs health status and stress levels, I measured mitochondrial membrane potential (MMP) (**Figure 32**). The data clearly indicate an significant increase of MMP in NT and T HCV-infected patients compared to HC (p=0,007). After DAAs therapy (at SVR 12 and 24 week) MMP levels seem to slowly normalize, although not to physiological levels.

These data indicate that HCV infection deeply alters M-MDSCs metabolic status, and these dysfunctions may persist also after viral clearance.

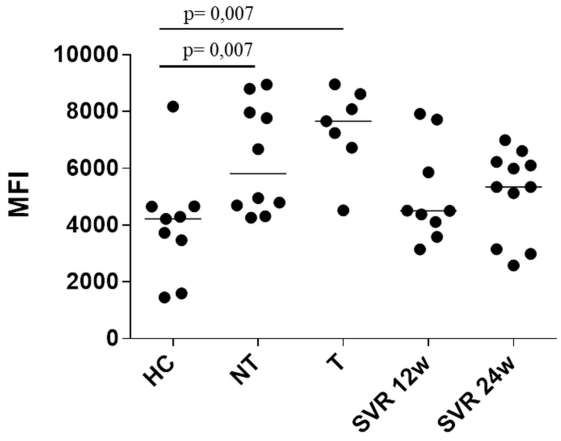

Figure 32: Mitochondrial membrane potential levels in M-MDSC expressed as mean fluorescents intensity (MFI) in: not treated patients (NT, n=10), patients treated with DAAs therapy (T, n=7), patients pharmacologically (after DAAs therapy) cured after 12 weeks (SVR 12week, n=9) and 24 weeks (SVR 24week, n=11) and healthy controls (HC, n=9). [*Mann-Whitney test*].

4.10 miRNAs expression in plasma samples of HCV-infected patients

Relying on the recent studies present in literature, for my thesis I have also analysed the expression of miRNA-122, miRNA-196b, miRNA-29a and miRNA-21 in plasma of 5 healthy donors and 45 HCV-infected patients. The patients selected for this analysis include the following (**Table 5**):

- 6 untreated (NT) subjects,

- 20 subjects treated with IFN-free therapy (3D Abbvie: ombitasvir + ritonavir + paritaprevir + dasabuvir + ribavirin) [n=10 during therapy (T) and n=10 pharmacologically cured (PC)],
- 6 subjects treated with IFN-based therapy (Peg-interferon + ribavirin + Telaprevir) [n=3 during therapy (T) and n=3 pharmacologically cured (PC)],
- 10 subjects treated with IFN-free therapy (sofosbuvir + ribavirin) [n=5 during therapy (T) and n=5 pharmacologically cured (PC)]
- 1 relapser (sofosbuvir + ribavirin)
- 2 spontaneously cured (SC)

The analysis was performed by Exiqon (Denmark), as detailed in the Materials and Methods section.

Figure 33 shows the heat map diagram and hierarchical clustering of both miRNAs and samples. In the heat map, each row represents one miRNA and each column one sample. The colour scale at the bottom of the diagram illustrates the expression level of microRNA across all samples: the red colour means expression level above the mean, the green colour an expression lower than the mean and the black colour an intermediate expression. At the left and on the top, there is the microRNA-clustering tree.

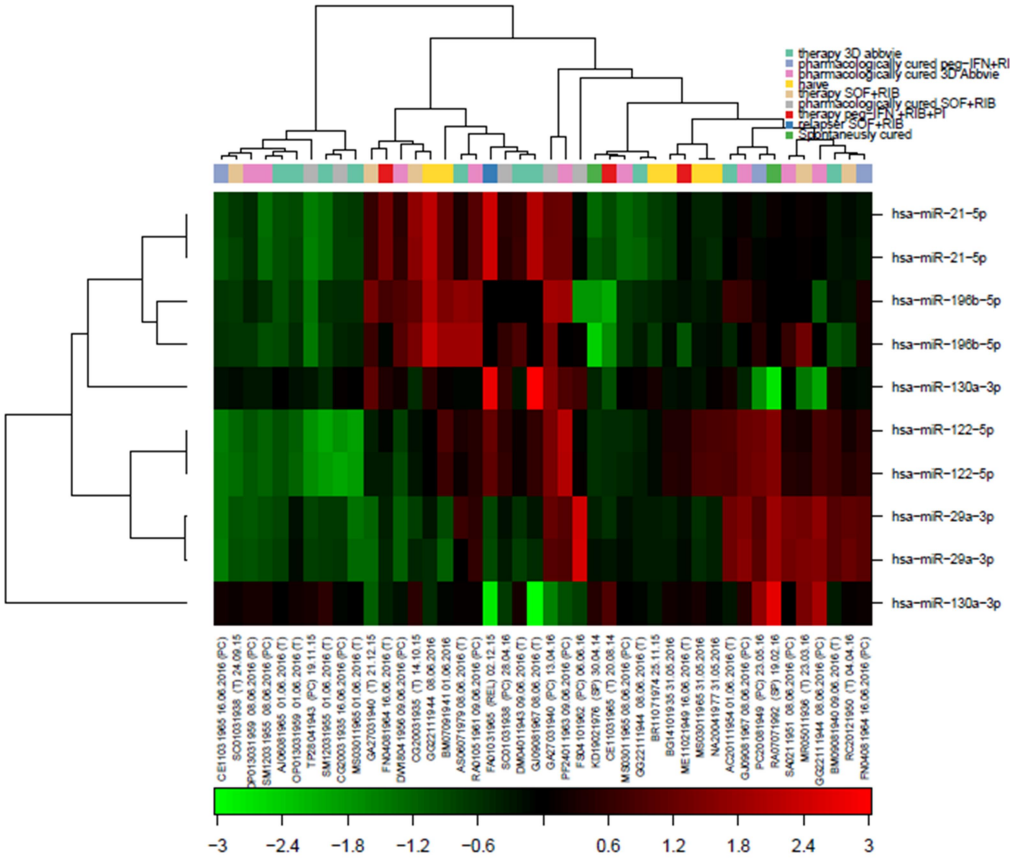

Figure 33: Heat map and hierarchical clustering. All 45 patients were classified based on their status. Patients during therapy: Peg-IFN+RBV (red), sofosbuvir + ribavirin (light brown) and 3D Abbvie (green water). Patients pharmacologically cured after the treatment with: Peg-IFN+RBV (violet), sofosbuvir + ribavirin (gray) and 3D Abbvie (fuchsia). Finally, untreated patients (NT) (yellow), one relapser after sofosbuvir + ribavirin therapy (blue) and two patients who cleared spontaneously the infection (green).

The samples did not cluster in specific groups. In particular, significant differences were observed only in the following comparisons: spontaneously cured vs NT (**Table 8**), relapser (Sofosbuvir + Ribavirin) vs NT (**Table 9**) and patients during 3D Abbvie therapy (Ombitasvir + Ritonavir + Paritaprevir + Dasabuvir + Ribavirin) vs NT (**Table 10**).

In the **Table 8**, the spontaneously cured (SC) group was compared to NT controls. In spontaneously cured volunteers, the expression of miRNA-196b and miRNA-21 decreased more than two-fold compared to NT. In contrast, the expression of miRNA-29a increased more than two-fold.

Table 8: Differentially expressed microRNAs in spontaneously cured patients vs NT patients

miRNA	Average dCq Patients SC (n=2)	Average dCq Patients NT (n=5)	Fold change
miRNA-196b-5p	-8.2	-3.7	-22
miRNA-196b-5p	-7.1	-3.4	-13
miRNA-29a-3p	2.0	-0.043	4.1
miRNA-29a-3p	2.0	0.19	3.5
miRNA-21-5p	5.6	6.9	-2.4
miRNA-21-5p	5.6	6.7	- 2.2
miRNA-130a-3p	-0.16	0.050	-1.2
miRNA-130a-3p	0.16	-0.050	1.2
miRNA-122-5p	2.4	2.3	1.0
miRNA-122-5p	2.5	2.5	1.0

In **Table 9**, the expression of miRNA-122 and miRNA-21 increased more than two-fold in the relapser (Sofosbuvir+Ribavirin)compared to the NT group.

Table 9: Differentially expressed microRNAs in the relapser after sofosbuvir +ribavirin therapy vs NT patients

miRNA	Average dCq Patients relapse (n=1)	Average dCq Patients NT (n=5)	Fold change
miRNA-21-5p	11	6.9	15
miRNA-21-5p	11	6.7	15
miRNA-122-5p	4.5	2.5	4.0
miRNA-122-5p	4.2	2.3	3.8
miRNA-29a-3p	-0.56	-0.043	-1.4
miRNA-29a-3p	-0.30	0.19	-1.4
miRNA-130a-3p	0.39	0.050	1.3
miRNA-130a-3p	-0.39	-0.050	-1.3
miRNA-196b-5p	ND*	-3.4	ND*
miRNA-196b-5p	ND*	-3.7	ND*

*ND, not detected

Finally, in the group of patients during 3D Abbvie therapy the expression of miRNA-122 showed a more that two-fold decrease compared to controls.

Table 10: Differentially expressed microRNAs in patients during 3D Abbvie therapy vs NT patients

miRNA	Average dCq Patients under 3D Abbvie	Average dCq naive	Fold change
miRNA-122-5p	-0.14	2.3	-5.6
miRNA-122-5p	0.0054	2.5	-5.4

5. DISCUSSION

MDSCs play a pivotal role in suppressing host immunity. In particular, in the last years, few studies in vitro suggested that hepatitis C virus promotes the accumulation of monocytic-MDSCs (M-MDSCs) that have the ability to suppress the functionality of some immune cells, such as T and NK lymphocytes. In this project, I investigated the correlation between the presence of M-MDSCs and the persistence of HVC infection and its immunological consequences (i.e. immune activation). In addition, I examined the expression of miRNA-122, miRNA-196b, miRNA-29a and miRNA-21 as possible biomarkers predictors for progression of disease and/or cure. Finally, I assessed whether IFN-based and IFN-free antiviral therapies could restore HCV-induced immune dysfunctions.

The results of this study revealed the accumulation of M-MDSCs in individuals with HCV-chronic infection compared to healthy controls, consistently with other studies that observed increase in M-MDSC numbers in untreated HCV-infected individuals (**Figure 12**) (Ren J.P. et al., 2016; Cai W.et al., 2013; Ning G. et al., 2015). In contrast, Nonnenmann J. and colleagues (2014), did not find any significant difference between the percentage of MDSCs in the peripheral blood of HCV patients and healthy donors, highlighting how much controversial is the role of these cells in hepatitis C.

It has been previously reported that the frequency of M-MDSCs is correlated with the clinical biochemical parameters of HCV patients, including HCV viral load and the level of ALT and AST which reflect liver injury (Cai W. et al., 2013; Zeng Q. et al., 2014). However, consistently with other reports, (Liu Y. et al., 2014; Ning G. et al., 2015; Nonnenmann J. et al., 2014), I did not observe such correlations between the frequency of M-MDSCs and HCV RNA, AST, or ALT. This suggests that the disease stage and severity is not associated with the increased number of M-MDSCs observed during HCV infection.

Notably, I also observed higher percentages of M-MDSCs in treated and pharmacologically cured patients compared to healthy controls, irrespective of the type of therapy (IFN-based therapy or DAAs). This suggests that HCV antiviral treatments do not affect M-MDSC numbers, even if this is measured 12 weeks after viral clearance. These results are partially discordant with a previous study describing a decreased frequency of M-MDSCs after 4 week of treatment with IFN-based treatments (Liu Y. et al., 2014).

However, analyzing a small longitudinal cohort of patients treated only with DAAs, whose samples were collected at two time points after sustained virologic response (12 week and 24 week), I observed that the frequency of M-MDSC cells decreased significantly ($p<0,0001$) from 3 months to 6 months from virus clearance (**Figure 23**). A further evaluation of the data pointed out a

correlation between the number of M-MDSCs after SVR 12 week and their proportional decrease at SVR 24 week, suggesting that the restoration of M-MDSCs numbers takes time, occurring 6 months after the viral clearance. To better understand this phenomenon I measured the cytokines profile in the plasma of the same donors. This analysis revealed a significant downregulation of GM-CSF and IL-10 from week 12 to 24. Several studies have shown that both GM-CSF and IL-10 are involved in the accumulation and activation of M-MDSCs (Trikha P. and Carson III W.E., 2014; Lechner M.G. et al., 2010). These data suggest that M-MDSC numbers decrease after 3 months of therapy due to the loss of the two molecules (GM-CSF and IL-10) that are sustaining their accumulation.

To measure if the quantitative alteration of M-MDSCs occurring after HCV infection and DAAs therapy was mirrored by a qualitative ones, I then measured the production of ROS, which are suppressive mechanism put in place by M-MDSCs (Gabrilovich D.I. and Nagaraj S., 2009), and their metabolic state measured by MMP. The data suggest that ROS production is increased in untreated HCV-infected patients compared to patients at SVR 24 week (p=0,034), but they are resorted to normal levels suddenly after therapy initiation. In contrast, HCV infection strongly alters MMP, which in only partially normalized by DAAs therapy, indicating that HCV infection deeply alter M-MDSCs metabolic status, and these dysfunctions may persist also after viral clearance. As this is the first work assessing metabolic alterations of M-MDSCs during HCV infection, further studies are needed to deepen this aspect.

To better define the immunologic determinants of HCV clearance and persistence, I examined also the phenotype of circulating T-cells. In particular, it is interesting to note the increase of the both $CD4^+$ and $CD8^+$ central memory T cells in NT HCV-infected patients (**Figure 27**), which is not restored after viral clearance, and the increased activation of memory $CD8^+$ T cell subsets (CM, EM and EMRA) in all study groups, even 6 months after therapy initiation (**Figure 28**). These data confirm previous works describing the immune activation of T-lymphocytes during HCV infection (Neumann-Haefelin C. and Thiemme R., 2013; Kumthip K. and Maneekarn N., 2015), and suggest that DAAs therapy only partially reverts this phenomenon.

Considering the exhaustion status of T cells, only CM $CD8^+$ T cells express high levels of PD1 in non-treated HCV infection (**Figure 29**), these are the first data that considering the PD1 expression in the different T cell subsets (CM, EM and EMRA).

Finally, the frequency of circulating Treg in HCV non-treated patients (NT) was significantly higher compared to healthy controls (p=0,049) according to studies suggesting Tregs as one of the major responsible for the dysfunctions of HCV-specific T cells in chronically infected patients (Accapezzato D. et al., 2004;

Cabrera R. et al., 2004). Of note, their numbers persisted elevated also at SVR 24 week, suggesting that DAAs therapy does not have effects on this cell types.

Nowadays, we know that miRNAs are able to modulate various biological process, as regulators of gene expression. Therefore, a preliminary analysis of the expression of few miRNAs (miRNA-122, miRNA-196b, miRNA-29a and miRNA-21), was carried out for 45 HCV-infected patients in order to investigated a possible role of these small non-coding RNAs in HCV infection. The preliminary results indicate that they are differentially expressed mostly between patients who spontaneously cleared infection (**Table 8**) and relapser (**Table 9**) as compared to not treated patients. The relapser patients are patients with undetectable levels of HCV RNA in the serum during treatment but become positive for HCV RNA at the end of this, therefore not surprised that miRNA-21 and miRNA-122 were highly expressed. miR-21 was shown to target myeloid differentiation factor 88 (MyD88) and interleukin-1 receptor-associated kinase 1 (IRAK1), which are involved in type I IFN production induced by the HCV, this subsequently leads to repressed IFN mediated antiviral response, thereby promoting viral replication (Chen Y. et al., 2013). Liver specific miR-122 that binds 5' UTR of HCV genomic RNA moderately stimulating viral protein translation and protects the uncapped HCV RNA genome from degradation (Sedano C.D. et al., 2014). However, these results require further investigation.

In summary, the study demonstrates that M-MDSCs are deeply altered by HCV infection, both quantitatively and qualitatively, and this is part of a more general phenomenon of HCV-induced immune dysregulation involving also the T cell subset. Notably, DAA-based therapies only partially, and slowly, restore these immunological alterations. This may also partly explain the increased incidence of hepatic tumors in DAA-treated individuals (Grandhe S. and Frenette C.T., 2017), whose immune functions remain altered and inflammation levels higher also several months after viral clearance.

6. REFERENCES

1. Accapezzato D., Francavilla S., Paroli M., Casciaro M., Chircu L.V., Cividini A, Mondelli M.U., Barnaba V. (2004) Hepatic expansion of a virus-specific regulatory $CD8^+$ T cell population in chronic hepatitis C virus infection. *The journal of Clinical Investigation* 113:963–972
2. Barth H. (2015) Hepatitis C virus: Is it time to say goodbye yet? Perspectives and challenges for the next decade. *World Journal of hepatology* 7:725-737
3. Bowen D.G. and Walker C.M. (2005) The origin of quasispecies: cause or consequence of chronic hepatitis C viral infection? *Journal of hepatology* 42:408-417
4. Bronte V., Brandau S., Chen S., Colombo M.P., Frey A.B., Greten T.F., Mandruzzato S., Murray P.J., Ochoa A., Ostrand-Rosenberg S., Rodriguez P.C., Sica A. Umansky V., Vonderheide R.H., Gabrilovich D.I. (2016) Recommendations for myeloid-derived suppressor cell nomenclature and characterization standards. *Nature Communications* 7:12150
5. Bukh J. (2016) The history of hepatitis C virus (HCV): Basic research reveals unique features in phylogeny, evolution and the viral life cycle with new perspectives for epidemic control. *Journal of hepatology* 65:S2-S21
6. Burchill M.A., Golden-Mason L., Wind-Rotolo M., Rosen H.R. (2015) Memory re-differentiation and reduced lymphocyte activation in chronic HCV-infected patients receiving direct-acting antivirals. *Journal of viral hepatitis* 22:983-991
7. Cabrera R., Tu Z., Xu Y., Firpi R.J., Rosen H.R., Liu C., Nelson D.R. (2004) An immunomodulatory role for CD4(+)CD25(+) regulatory T lymphocytes in hepatitis C virus infection. *Hepatology* 40:1062-1071
8. Cai W., Qin A., Guo P., Yan D., Hu F., Yang Q., Xu M., Fu Y., Zhou J., Tang X. (2013) Clinical significance and functional studies of myeloid-derived suppressor cells in chronic hepatitis C patients. *Journal of clinical immunology* 33:798-808
9. Cheng J.C., Yeh Y.J., Tseng C.P., Hsu S.D., Chang Y.L., Sakamoto N., Huang H.D. (2012) Let-7b is a novel regulator of hepatitis C virus replication. *Cellular and molecular life sciences* 69:2621-2633
10. Chen S., Zhang Y., Kuzel T.M., Zhang B. (2015) Regulating tumor myeloid-derived suppressor cells by microRNAs. *Cancer cell microenvironment* 2:637
11. Chen X. (2009) MicroRNA signature in liver diseases. *World Journal Gastroenterology* 15:1665-1672

12. Chen Y., Chen J., Wang H., Shi J., Wu K., Liu S., Liu Y., Wu J. (2013) HCV-induced miR-21 contributes to evasion of host immune system by targeting MyD88 and IRAK1. *PLoS Pathogens* 9:e1003248
13. Chiu D.K., Tse A.P., Xu I.M., Di Cui J., Lai R.K., Li L.L., Koh H.Y., Tsang F.H., Wei L.L., Wong C.M., Ng I.O., Wong C.C. (2017) Hypoxia inducible factor HIF-1 promotes myeloid-derived suppressor cells accumulation through ENTPD2/CD39L1 in hepatocellular carcinoma. *Nature communications* 8:517
14. Chung R.T., Gale M., Polyak S.J., Lemon S.M. Liang T.J., Hoofnagle H. (2008) Mechanisms of action of interferon and ribavirin in chronic hepatitis C: Summary of a workshop. *Hepatology* 47: 306-320
15. Condamine T. and Gabrilovich D.I. (2011) Molecular mechanisms regulating myeloid-derived suppressor cell differentiation and function. *Trend immunology* 32:19-25
16. Condamine T., Dominguez G.A., Youn J.I., Kossenkov A.V., Mony S., Alicea-Torres K., Tcyganov E., Hashimoto A., Nefedova Y., Lin C., Partlova S., Garfall A., Vogl D.T., Xu X., Knight S.C., Malietzis G., Lee G.H., Eruslanov E., Albelda S.M., Wang X., Mehta J.L., Bewtra M., Rustgi A., Hockstein N., Witt R., Masters G., Nam B., Smirnov D., Sepulveda M.A., Gabrilovich D.I. (2016) Lectin-type oxidized LDL receptor-1 distinguishes population of human polymorphonuclear myeloid-derived suppressor cells in cancer patients. *Science immunology* 1:aaf8943
17. Damuzzo V., Pinton L., Desantis G., Solito S., Marigo I., Bronte V., Mandruzzato S. (2015) Complexity and challenges in defining myeloid-derived suppressor cells. *Cytometry Part B clinical cytometry* 88:77-91
18. Daw M.A., El-Bouzedi A.A., Ahmed M.O., Dau. A.A. Agnan M.M., Drah A.M. (2016) Geographic integration of hepatitis C virus: A global threat. *World Journal Virology* 5:170-182.
19. Delegan L., Neyts J., Vliegen I., Abrignani S., Neddermann P., De Francesco R. (2013) Hepatitis C virus-specific directly acting antiviral drugs. *Current topics in microbiology and immunology* 369:289-320
20. Dimeloe S., Burgener A.V., Grählert J., Hess C. (2016) T-cell metabolism governing activation, proliferation and differentiation; a modular view. *Immunology* 150:35-44
21. Dorhoi A. and Du Plessis N. (2018) Monocytic Myeloid-Derived Suppressor Cells in Chronic Infections. *Frontiers in immunology* 8:1895
22. Duan X., Li S., Li Y., Zeng P., Yang C., Chen L. (2013) The role of microRNA in hepatitis C virus replication. *Journal of clinical and translational hepatology* 1:125-130

23. Elmasry, S., Wadhwa, S., Bang, B.R., Bang B.R., Cook L., Chopra S., Kanel G., Kim B., Harper T., Feng Z., Jerome K.R., Kahn J.A., Saito T. (2017) Detection of occult hepatitis C virus infection in patients who achieved a sustained virologic response to direct-acting antiviral agents for recurrent infection after liver transplantation. *Gastroenterology* 152:550–553.
24. Elberry M.H., Darwish NH.E., Mousa S.A. (2017) Hepatitis C virus management: potential impact of nanotechnology *Virology journal* 14:88
25. Enomoto H., Nishikawa H., Ikeda N., Aizawa N., Sakai Y., Yoh K., Takata R., Hasegawa K., Nakano C., Nishimura T., Ishii A., Takashima T., Iwata Y., Iijima H., Nishiguchi S. (2016) Improvement in the Amino Acid Imbalance in Hepatitis C Virus Infected Patients After Viral Eradication by Interferon Treatment. *Hepatitis Monthly* 16:e35824
26. Fallahi P., Ferri C., Ferrari S.M., Corrado A., Sansonno D., Antonelli A. (2012) Cytokines and HCV-related disorders. *Clinical and developmental immunology* 468107
27. Fournier C., Duverlie G, Castelain S. (2013) Are trans-complementation systems suitable for hepatitis C virus life cycle studies? *Journal of viral hepatitis* 20:225-233
28. Friebe P. and Bartenschlager R. (2009) Role of RNA structures in genome terminal sequences of the hepatitis C virus for replication and assembly. *Journal of virology* 83:11989-11995
29. Gabrilovich D.I. and S. Nagaraj. (2009) Myeloid-derived suppressor cells as regulators of the immune system. *Nature reviews* 9:162-174
30. Gabrilovich D.I. (2017) Myeloid-Derived Suppressor Cells. *Cancer immunology research* 5:3-8
31. Gimeno-Ballester V., Buti M., San Miguel R., Riveiro M., Esteban R. (2017) Interferon-free therapies for patients with chronic hepatitis C genotype 3 infection: A systematic review. *Journal of viral hepatitis* 24:904-916
32. Goh C., Narayanan S., Hahn Y. (2013) Myeloid derived suppressor cells: the dark knight or the joker in viral infections? *Immunological Reviews* 255:210-221
33. Goh C., Roggerson K., Lee K., Golden-Mason L., Rosen H.R., Hahn Y.S. (2016) Hepatitis C virus-induced myeloid-derived suppressor cells suppress NK cell IFN-γ production by altering cellular metabolism via arginase-1. *The journal of immunology* 196:2283-2292
34. Grandhe S. and Frenette C.T. (2017) Occurrence and Recurrence of Hepatocellular Carcinoma After Successful Direct-Acting Antiviral

Therapy for Patients With Chronic Hepatitis C Virus Infection. *Gastroenterology & Hepatology* 13:421–425

35. Guglietta S., Garbuglia A.R., Salichos L., Ruggeri L., Folgori A., Perrone M.P., Camperio C., Mellace V., Maio G., Maio P., Capobianchi M.R., Spada E., Gargano N., Scottà C., Piccolella E., Del Porto P. (2009) Impact of viral selected mutations on T cell mediated immunity in chronically evolving and self-limiting acute HCV infection. *Virology* 386:398-406
36. Gurianova V., Stroy D., Ciccocioppo R., Gasparova I., Petrovic D., Soucek M., Dosenko V., Kruzliak P. (2015) Stress response factors as hub-regulators of microRNA biogenesis: implication to the diseased heart. *Cell biochemistry and function* 33:509-518
37. Haile L.A., Gamrekelashvili J., Manns M.P., Korangy F., Greten T.F. (2010) CD49d is a new marker for distinct myeloid-derived suppressor cell subpopulations in mice. *Journal of immunology* 185:203-210
38. Hajarizadeh B., Grebely J. and Dore G.J. (2013) Epidemiology and natural history of HCV infection. *Nature Review Gastroenterology & Hepatology* 10:553-562
39. Halfon P. and Locarnini S. (2011) Hepatitis C virus resistance to protease inhibitors. *Journal of hepatology* 55:192-206
40. Hamamoto I., Nishimura Y., Okamoto T., Aizaki H., Liu M., Mori Y., Abe T., Suzuki T., Lai M.M., Miyamura T., Moriishi K., Matsuura Y. (2005) Human VAP-B is involved in hepatitis C virus replication through interaction with NS5A and NS5B. *Journal of virology* 79:13473-13482
41. Hammerich L. and Tacke F. (2015) Emerging roles of myeloid derived suppressor cells in hepatica inflammation and fibrosis. *World Journal of Gastrointestinal Pathophysiology* 6:53-50
42. Heim M.H. (2013) 25 years of interferon-based treatment of chronic hepatitis C: an epoch coming to an end. *Nature Reviews* 13:535-542
43. Heim. M.H. and Thiemme R. (2014) Innate and adaptive immune responses in HCV infections. *Journal of hepatology* 61:14-25
44. Hengst J., Falk C.S., Schlaphoff V., Deterding K., Manns M.P., Cornberg M., Wedemeyer H. (2016) Direct-Acting Antiviral-Induced Hepatitis C Virus Clearance Does Not Completely Restore the Altered Cytokine and Chemokine Milieu in Patients With Chronic Hepatitis C. *Journal of infectious diseases* 214:1965-1974
45. Hoechst B., Ormandy L.A., Ballmaier M., Lehner F., Kruger C., Manns M.P., Greten T.F., Korangy F. (2008) A new population of myeloid-derived suppressor cells in hepatocellular carcinoma patients induces $CD4^{+}CD25^{+}Foxp3^{+}$ T cells. *Gastroenterology* 135:234-243

46. Hoffmann T.W., Gilles D., Abderrahmane B. (2012) MicroRNAs and hepatitis C virus: Toward the end of miR-122 supremacy *Virology Journal* 9:109
47. Horsley-Silva J.L. and Vargas H.E. (2017) New Therapies for Hepatitis C Virus Infection. *Gastroenterology and hepatology* 13:22-31
48. Huang B., Ping-Ying P., Li Q., Sato A.I.,. Levy D. E., Bromberg J., Divino C.M., Chen S.H. Gr-1^{+}CD115^{+} Immature Myeloid Suppressor Cells Mediate the Development of Tumor-Induced T Regulatory Cells and T-Cell Anergy in Tumor-Bearing Host. *Cancer Research* 66:1123-1131
49. Huang L., , Sineva E.V., Hargittai M.R., Sharma S.D., Suthar M., Raney K.D., Cameron C.E. Purification and characterization of hepatitis C virus non-structural protein 5A expressed in Escherichia coli. (2004) *Protein expression and purification* 37:144-153
50. Huang L., Hwang J., Sharma S.D., Hargittai M.R., Chen Y., Arnold J.J., Raney K.D., Cameron C.E. (2005) Hepatitis C virus nonstructural protein 5A (NS5A) is an RNA-binding protein. *Journal of biological chemistry* 280:36417-36428
51. Jadoon S.A., Ahmed A., Jehangiri A., Ahmad N. (2015) Effect of standard interferon and ribavirin on leukocyte count. *Journal of Ayub Medical College Abbottabad* 27(2)
52. Khan A.G., Whidby J., Miller M.T., Scarborough H., Zatorski A.V., Cygan A., Price A.A., Yost S.A., Bohannon C.D., Jacob J., Grakoui A., Marcotrigiano J. (2014) Structure of the core ectodomain of the hepatitis C virus envelope glycoprotein 2. *Nature* 509:381-384
53. Kim V.N. (2005) MicroRNA Biogenesisis: coordinated cropping and dicing. *Nature reviews* 9:376-385
54. Kotsakis A., Harasymczuk M., Schilling B., Georgoulias V., Argiris A., Whiteside T.L. (2012) Myeloid-derived suppressor cell measurements in fresh and cryopreserved blood samples. *Journal Immunology methods* 381:14-22
55. Koutsoudakis G., Pérez-Del-Pulgar S., Forns X. (2017) Occult Hepatitis C Virus Infection: Are We Digging Too Deep? *Gastroenterology* 152:472-474
56. Kumthip K. and Mannekarn N. (2015) The role of HCV proteins on treatment outcomes. *Virology Journal* 12:217
57. Langhans B., Nischalke H.D., Krämer B., Hausen A., Dold L., van Heteren P., Hüneburg R., Nattermann J., Strassburg C.P., Spengler U. (2017) Increased peripheral CD4^{+} regulatory T cells persist after successful direct-acting antiviral treatment of chronic hepatitis C. *Journal of hepatology* 66:888-896

58. Larrubia J.R., Moreno-Cubero E., Miquel J., Sanz-de-Villalobos E. (2015) Hepatitis C virus-specific cytotoxic T cell response restoration after treatment-induced hepatitis C virus control. *World journal of gastroenterology* 21:3480-3491
59. Lassmann B., Arumugaswami V., Chew K.W., Lewis M.J. (2013) A new system to measure and compare hepatitis C virus replication capacity using full-length, replication competent viruses. *Journal of Virological Methods* 194:82-88
60. Lauer G.M. (2013) Immune responses to hepatitis C virus (HCV) infection and the prospects for an effective HCV vaccine or immunotherapies. *The journal of infectious diseases* Suppl 1:S7-S1.
61. Li L., Zhang J., Diao W., Wang D., Wei Y., Zhang C., Zen Ke (2014) MicroRNA-155 and microRNA-21 promote the expansion of functional myeloid-derived suppressor cells. *The journal of immunology* 192:1034-1043
62. Liu C., Wang Y., Wang C., Feng P., Ko H., Liu Y., Wu Y., Chu Y., Chung F., Lee K., Lin S., Lin H., Wang C., Yu C., Kuo H. (2010) Population alternations of L-arginase and inducible nitric oxide synthase-expressed $CD11b^{+}/CD14^{-}/CD15^{+}/CD33^{+}$ myeloid-derived suppressor cells and $CD8^{+}$ T lymphocytes in patients with advanced-stage non-small cell lung cancer. *Journal of Cancer Research and Clinical Oncology* 136:35-45
63. Liu Y., She L., Wang X., Zhang G., Yan Y., Lin C., Zhao Z., Gao Z. (2014) Expansion of myeloid-derived suppressor cells from peripheral blood decrease after 4-week antiviral treatment in patients with chronic hepatitis C. *Internal journal of clinical and experimental medicine* 7:998-1004
64. Manns M.P., Buti M., Gane E., Pawlotsky J.M., Razavi H., Terrault N., Younossi Z. (2017) Hepatitis C virus infection. *Nature reviews diseases primers* 3:17006
65. Mandruzzato S., Solito S., Falisi E., Francescato S., Chiarion-Sileni V., Mocellin S., Zanon A., Rossi C.R., Nitti D., Bronte V., Zanovello P. (2009) $IL4Ralpha^{+}$ myeloid-derived suppressor cell expansion in cancer patients. *The journal of immunology* 182:6562-6568
66. Mandruzzato S., Brandau S., Britten C.M., Bronte V., Damuzzo V., Gouttefangeas C., Maurer D., Ottensmeier C., van der Burg S.H., Welters M.J., Walter S. (2016) Toward harmonized phenotyping of human myeloid-derived suppressor cells by flow cytometry: results from an interim study. *Cancer immunology immunotherapy* 65:161-169
67. Macdonald A. and Harris M. (2004) Hepatitis C virus NS5A: tales of a promiscuous protein. *Journal of general virology* 85:2485-2502

68. Maue A.C., Yager E.J., Swain S.L., Woodland D.L., Blackman M.A., Haynes L. (2009) T-cell immunosenescence: lessons learned from mouse models of aging. *Trends immunology* 30:301-305
69. Medina-Echeverz J., Eggert T., Han M., Greten T.F. (2015) Hepatic myeloid-derived suppressor cells in cancer. *Cancer Immunology immunotherapy* 64:931-940
70. Messina J.P., Humphreys I., Flaxman A., Brown A., Cooke G.S., Pybus O.G., Barnes E. (2015) Global distribution and prevalence of hepatitis C virus genotypes. *Hepatology* 61:77-87
71. Millrud C.R., Bergenfelz C., Leandersson K. (2017) On the origin of myeloid-derived suppressor cells. *Oncotarget* 8:3649-3665
72. Moradpour D., Penin F., Rice C. (2007) Replication of hepatitis C virus. *Nature Reviews* 5:453-463
73. Moradpour D. and Penin F. (2013) Hepatitis C virus proteins: from structure to function. *Current Topics in Microbiology and Immunology* 369:113-142
74. Neumann-Haefelin C. and Thiemme R. (2013) Adaptive immune responses in hepatitis C virus infection. *Current Topics in Microbiology and Immunology* 369:243-262
75. Ning G., She L., Lu L., Lu Y., Zeng Y., Yan Y., Lin C. (2015) Analysis of monocytic and granulocytic myeloid-derived suppressor cells subsets in patients with hepatitis C virus infection and their clinical significance. *BioMed Research International* Vol 15
76. Nonnenmann J., Stirner R., Roider J., Jung M.C., Schrodl K., Bogner J.R., Draenert R. (2014) Lack of significant elevation of myeloid-derived suppressor cells in peripheral blood of chronically HCV infected individuals. *Journal of Virology* 88:7678-7682
77. Ostrand-Rosenberg S. and Sinha P. (2009) Myeloid-derived suppressor cells: Linking inflammation and cancer. *The Journal of Immunology* 182:4499-4506
78. Pang X., Song H., Zhang Q., Tu Z., Niu J. (2016) Hepatitis C virus regulates the production of monocytic myeloid-derived suppressor cells from peripheral blood mononuclear cells through PI3K pathway and autocrine signaling. *Clinical immunology* 164:57-64
79. Papagno L., Spina C.A., Marchant A., Salio M., Rufer N., Little S., Dong T., Chesney G., Waters A., Easterbrook P., Dunbar P.R., Shepherd D., Cerundolo V., Emery V., Griffiths P., Conlon C., McMichael A.J., Richman D.D., Rowland-Jones S.L., Appay V. (2004) Immune activation and $CD8^+$ T-cell differentiation towards senescence in HIV-1 infection. *PLoS biology* 2:E20

80. Pawlotsky J.M. (2016) Hepatitis C Drugs: Is Next Generation the Last Generation? *Gastroenterology* 151:587-90
81. Pecheur E.I. (2012) Lipoprotein receptors and lipid enzymes in hepatitis C virus entry and early steps of infection. *Scientifica* 2012:709-853
82. Pham T.N., Coffin C.S., Michalak T.I. (2010) Occult hepatitis C virus infection: what does it mean? *Liver international* 30:502-11
83. Pieczenik S.R. and Neustadt J. (2007) Mitochondrial dysfunction and molecular pathways of disease. *Experimental and molecular pathology* 83:84-92
84. Poordad F., Hezode C., Trinh R, Kowdley K., Zeuzem S., Agarwal K., Shiffman M.L., Wedemeyer H., Berg K., Yoshida E.M., Forns X., Lovell S.S., Da-Silva-Tillmann B., Collins C., Campbell A. Podsadecki T., Bernstein B. (2014) ABT-450/r-ombitasvir and dasabuvir with ribavirin for hepatitis c with cirrhosis. *The New England journal of medicine* 370:1973-1982
85. Rajesh S., Sridhar P., Tews B.A., Fénéant L., Cocquerel L., Ward D.G., Berditchevski F., Overduin M. (2012) Structural basis of ligand interactions of the large extracellular domain of tetraspanin CD81. *Journal of Virology* 86:9606-9616
86. Reig M., Torres F., Mariño Z., Forns X., Bruix J. (2016) Reply to "Direct antiviral agents and risk for hepatocellular carcinoma (HCC) early recurrence: Much ado about nothing". *Journal of hepatology* 65:864-865
87. Ren J.P., Zhao J., Dai J., Griffin J.W.D., Wang L., Wu X.Y., Morrison Z.D. Li G.L., Gazzar M., Ning S.B., Moorman J.P., Yao Z.Q. (2016) Hepatitis C virus-induced myeloid-derived suppressor cells regulate T-cell differentiation and function via the signal transducer and activator of transcription 3 pathway. *Immunology* 148:377-386
88. Ren J.P., Wang L., Zhao J., Wang L., Ning S.B., El Gazzar M., Moorman J.P., Yao Z.Q. (2017) Decline of miR-124 in myeloid cells promotes regulatory T-cell development in hepatitis C virus infection. *Immunology* 150:213-220
89. Rodríguez P.C. and Ochoa A.C. (2008) Arginine regulation by myeloid derived suppressor cells and tolerance in cancer: mechanisms and therapeutic perspectives. *Immunological review* 222:180-191
90. Santos J.M.O., Gil da Costa R.M., Medeiros R. (2018) Dysregulation of cellular microRNAs by human oncogenic viruses - Implications for tumorigenesis. *Biochimica et Biophisica acta* 1861:95-105
91. Scagnolari C., Zingarello P., Vecchiet J., Selvaggi C., Racciatti D., Taliani G., Riva E., Pizzigallo E., Anonelli G. (2010) Differential expression of

interferon-induced microRNAs in patients with chronic hepatitis C virus infection treated with pegylated interferon alpha *Virology Journal* 7:311

92. Scheel T.K. and Rice C.(2013) Understanding the hepatitis C virus life cycle paves the way for highly effective therapies. *Nature Medicine* 19:837
93. Serti E., Chepa-Lotrea X., Kim Y.J., Keane M., Fryzek N., Liang T,J., Ghany M., Rehermann B. (2015) Successful Interferon-Free Therapy of Chronic Hepatitis C Virus Infection Normalizes Natural Killer Cell Function. *Gastroenterology* 149:190-200
94. Sedano C.D. and Sarnow P. (2014) Hepatitis C virus subverts liver-specific miR-122 to protect the viral genome from exoribonuclease Xrn2. *Cell Host & Microbe* 16:257–260
95. Shiryaev S.A., Cheltsov A.V., Strongin A.Y. (2012) Probing of exosites leads to novel inhibitor scaffolds of HCV NS3/4A proteinase. *Plos one* 7:e40029
96. Schoggins J.W. and Rice M. (2013) Innate immune responses to hepatitis C virus. *Current Topics in Microbiology and Immunology* 369:219-242
97. Singaravelu R., Desrochers G.F., Srinivasan P., O'Hara S., Lyn R.K., Müller R., Jones D.M., Russell R.S., Pezacki J.P. (2015) Soraphen A: A Probe for Investigating the Role of de Novo Lipogenesis during Viral Infection. *ACS infectious diseases* 1:130-134
98. Spaan M., Janssen H.L.A., Boonstra A. (2012) Immunology of hepatitis C virus infections. *Best practice & Research clinical gastroenterology* 26:391-400
99. Sohn W., Kim J., Kang S.H., Yang S.R., Cho J.Y., Cho H.C., Shim S.G., Paik Y.H. (2015) Serum exosomal microRNAs as novel biomarkers for hepatocellular carcinoma. *Experimental and molecular medicine* 47:e184
100. Solito S., Marigo I., Pinton L., Damuzzo V., Mandruzzato S., Bronte V. (2014) Myeloid-derived suppressor cell heterogeneity in human cancers. *Annals of the new york academy of sciences* 1319:47-65
101. Steinmann E., Brohm C., Kallis S., Bartenschlager R., Pietschmann T.(2008) Efficient trans-encapsidation of hepatitis C virus RNAs into infectious virus-like particles. *Journal of Virology* 82:7034-7046
102. Sforza F., Nicoli F., Gallerani E., Finessi V., Reali E., Cafaro A., Caputo A., Ensoli B., Gavioli R. (2014) HIV-1 Tat affects the programming and functionality of human $CD8^+$ T cells by modulating the expression of T-box transcription factors. *AIDS* 28:1729-1738
103. Syed G.H., Amako Y., Siddiqui A. 2010 Hepatitis C virus hijacks host lipid metabolism. *Trends in endocrinology and metabolism* 21:33-40
104. Tacke R.S., Lee H., Goh C., Courtney J., Polyak S.J., Rosen H.R., Hahn Y.S. (2012) Myeloid suppressor cells induced by hepatitis C virus suppress

T-cell responses through the production of reactive oxygen species. *Hepatology* 55:343-353

105. Talmadge J.E. and Gabrilovich D.I. (2013) History of myeloid-derived suppressor cells. *Nature reviews* 13:739-752
106. Thiemme R., Binder M., Bartenschlager R. (2012) Failure of innate and adaptive immune responses in controlling hepatitis C virus infection. *FEMS Microbiology Review* 36:663-683
107. Tian J., Rui K., Wang S. (2014) Roles of miRNAs in regulating the differentiation and maturation of myeloid-derived suppressor cells. *Medical hypotheses* 83: 151-153
108. Waring J.F., Dumas E.O., Abel S., Coakley, Coeh D.E., Davis J.W., Podsadecki T., Dutta S. (2016) Serum miR-122 may serve as a biomarker for response to direct acting antivirals: effect of paritaprevir/R with dasabuvir or ombbitasvir on miR-122 in HCV-infected subjects. *Journal of Viral Hepatitis* 23:96-104
109. Welzel T.M., Dultz G., Zeuzem S. (2014) Interferon-free antiviral combination therapies without nucleosidic polymerase inhibitors. *Journal of hepatology* 61:98-107
110. Xie K.L., Zhang Y.G., Liu J., Zeng Y., Wu H.(2014) MicroRNAs associated with HBV infection and HBV-related HCC. *Theranostics* 4:1176-1192
111. Xu J., Wu C., Che X., Wang L., Yu., Zhang T., Huang L., Li H., Tan., Wang C., Lin D. (2011) Circulating microRNAs, miR-21, miR-122 and miR-223, in patients with hepatocellular carcinoma or chronic hepatitis. *Molecular carcinogenesis* 50:136-142
112. Yamamoto M., Sakamoto N., Nakamura T., Itsui Y., Nakagawa M., Nishimura-Sakurai Y., Kakinuma S., Azuma S., Tsuchiya K., Kato T., Wakita T., Watanabe M. (2011) Studies on virus kinetics using infectious fluorescence-tagged hepatitis C virus cell culture. *Hepatology research* 41:258-269
113. Yau A.H.L.Y. and Yoshida E.M. (2014) Hepatitis C drugs: the end of the pegylated interferon era and the emergence of all-oral, interferon-free antiviral regimens: A concise review. *Cancer Journal Gastroenterol Hepatology* 28:445-451
114. Vukotic R., Di Donato R., Conti F., Scuteri A., Serra C., Andreone P. (2017) Secondary prophylaxis of hepatocellular carcinoma: the comparison of direct-acting antivirals with pegylated interferon and untreated cohort. *Journal of Viral Hepatitis* 24:13-16

115. Zeisel M.B., Fofana I., Fafi-Kremer S., Baumert T.F. (2011) Hepatitis C virus entry into hepatocytes: molecular mechanisms and targets for antiviral therapies. *Journal of hepatology* 54:566-576
116. Zeng Q., Yang B., Sun H., Feng G., Jin L., Zou Z., Zhang Z., Zhang L., Wang F. (2014) Myeloid-derived suppressor cells are associated with viral persistence and downregulation of TCR ζ chain expression on $CD8^+$ T cells in chronic hepatitis C patients. *Molecules and Cells* 37:66-73
117. Zhai N., Li H., Song H., Yang Y., Cui A., Li T., Niu J., Crispe I.N., Su L., Tu Z. (2017) Hepatitis C Virus Induces MDSCs-Like Monocytes through TLR2/PI3K/AKT/STAT3 Signaling. *Plos one* 12:e0170516
118. Zhang S., Ouyang X., Jiang X., Dayong G., Lin Y., Kong S.K., Xie W. (2015) Dysregulated serum microRNA expression profile and potential biomarkers in hepatitis C virus-infected patients. *International journal of medical sciences* 12:590-598
119. Zuniga E.I., Macal M., Lewis G.M., Harker J.A.(2015) Innate and Adaptive Immune Regulation During Chronic Viral Infections. *Annual review of virology* 2:573-597

7. RINGRAZIAMENTI

Finalmente si è concluso questo lungo e intenso progetto di studio!!!

Volevo per questo sentitatemente ringraziare:

Il mio supervisore la Professoressa Antonella Caputo per il tempo dedicatomi e gli insegnamenti che è riuscita a trasmettermi.

Il Proferssor Giorgio Palù per la possibilità e la motivazione nella realizzazione di questo studio.

Il Dottor Francesco Nicoli per avermi aiutata a vedere qualsiasi difficoltà in modo positivo, per la discussione scientifica e per tutte le ore passate al citofluorimetro!

La Dott.ssa Elke Erne, il Dottor Francesco Barbaro, la Dott.ssa Eleonora Castelli e le infermire di Malattie Infettive e Tropicali dell'Azienda Ospedaliera di Padova per l'immane lavoro di reclutamenti dei donatori.

La Dott.ssa Chiara Frasson per il supporto tecnico e la sua infinita disponibilità.

La Professoressa Susanna Mandruzzato e la Dott.ssa Laura Pinton per i preziosi consigli e supporto nel trattatamento delle MDSCs.

Tutti i ragazzi che negli anni si sono alternati nel laboratorio al piano terra, che hanno reso tutto più leggero e spensierato.

Mio padre e mia madre per il supporto datomi in tutti questi anni di studio.

Infine mio marito Claudio e i mie due piccolini Giacomo ed Edoardo…senza di voi nulla avrebbe senso.